International Journal of Control
Vol. 00, No. 00, Month 200x, 1–20

RESEARCH ARTICLE

Dynamic Positioning for an Underactuated Marine Vehicle using Hybrid Control

Dimitra Panagou[a]* and Kostas J. Kyriakopoulos[b]

[a] *Coordinated Science Laboratory, College of Engineering, Univ. of Illinois at Urbana-Champaign, USA*;
[b] *Control Systems Lab, School of Mechanical Engineering, National Technical Univ. of Athens, Greece*

(*Received 00 Month 200x; final version received 00 Month 200x*)

The increasing interest in autonomous marine systems and related applications has motivated, among others, the development of systems and algorithms for the dynamic positioning of underactuated marine vehicles (ships, surface vessels, underwater vehicles) under the influence of unknown environmental disturbances. In this paper we present a state feedback control solution for the navigation and practical stabilization of an underactuated marine vehicle under non-vanishing current disturbances, by means of hybrid control. The proposed solution involves a logic-based switching control strategy among simple state feedback controllers, which renders the position trajectories of the vehicle practically stable to a goal set around a desired position. The control scheme consists of three control laws; the first one is active out of the goal set and drives the system trajectories into this set, based on a novel dipolar vector field. The other two control laws are active in the goal set and alternately regulate the position and the orientation of the vehicle, so that the switched system is practically stable around the desired position. The overall system is shown to be robust, in the sense that the vehicle enters and remains into the goal set even if the external current disturbance is unknown, varying and only its maximum bound (magnitude) is given. The efficacy of the proposed solution is demonstrated through simulation results.

Keywords: underactuated marine vehicles; dynamic positioning; external disturbances; logic-based switching, hybrid control

1 Introduction

Guidance, navigation and control of marine vehicles (ships, surface vessels and underwater vehicles) has received great interest over the past twenty years, motivated in part by their extensive use in oil industry, in scientific explorations (e.g. in oceanographic, archeological and marine biology research), in search and rescue missions, surveillance and inspection tasks, etc.

The control design for *underactuated* marine vehicles, in particular, constitutes an interesting and challenging subset of the overall problem, and has been mainly motivated by the need for minimal vehicle design, fault tolerance and control under thruster failures, as well as by the navigation problem for specific classes of vehicles, such as torpedo-shaped Autonomous Underwater Vehicles (AUV). There are various reasons that justify the characterization of the underactuated control design as challenging, including: (i) the manifestation of second-order nonholonomic constraints, which dictate the non-existence of continuous, time invariant state feedback control laws (Brockett 1983), (ii) the highly nonlinear and coupled structure of the system dynamics, as well as (iii) the effect of external disturbances due to waves, currents and wind (for surface vessels). It is generally accepted that each of these parameters should be carefully taken into consideration during the control design, so that the resulting closed-loop system performs efficiently and reliably in real environmental conditions.

*Corresponding author. Email: dpanagou@illinois.edu

ISSN: 0020-7179 print/ISSN 1366-5820 online

DOI: 10.1080/0020717YYxxxxxxxx
http://www.informaworld.com

1.1 *Literature Survey*

Driven mainly by the vivid research activity on the control of underactuated systems, the stabilizing control design for underactuated marine vehicles has been addressed via methods and strategies that overcome the limitation induced by Brockett's condition. Pioneer work in this direction has appeared in (Wichlund et al. 1995), where a smooth state-feedback law stabilizes an underactuated ship to an equilibrium manifold, instead of an equilibrium point. Smooth, time-varying controllers which yield asymptotic stability to the origin are proposed in (Pettersen and Egeland 1999, Pettersen and Fossen 2000, Mazenc et al. 2002, Do et al. 2002, Dong and Guo 2005), whereas discontinuous, time-invariant controllers are proposed in (Reyhanoglu 1996, Fantoni et al. 2000, Aguiar and Pascoal 2001, Ghommam et al. 2006, Cheng et al. 2002). More recently, the increasing research interest in hybrid systems and control has resulted in the formulation of hybrid control solutions, see for instance (Kim et al. 2002, Aguiar and Pascoal 2002, Greytak and Hover 2008, Ma 2009); in these contributions, a proper switching logic among suitably defined state feedback control laws yields asymptotic stability for various models of underactuated marine vehicles.

Very much related to the context of stabilizing control is the problem of *dynamic positioning* for underactuated marine vehicles. For a recent survey on dynamic positioning control systems the reader is referred to (Sørensen 2011). Briefly, the term dynamic positioning has been traditionally used to describe the process of automatically maintaining the position and heading of the vehicle by means of its own propellers and thrusters, only.[1] Therefore, the high-level dynamic positioning control problem reduces into finding a feedback control law that (ideally) asymptotically stabilizes both position and orientation to desired constant values.

Nevertheless, the effect of environmental (external) disturbances on the vehicle, which mainly arises due to waves, currents and the wind, in principle serves as a non-vanishing perturbation at the desired configuration; consequently, only practical stability can be ensured in practice. External disturbances due to waves and wind are dominating in the case of ships and surface vessels, whereas the motion of a fully submerged underwater vehicle is mostly affected by current disturbances. The aforementioned studies do not take into account the influence of environmental disturbances. To the best of our knowledge, pioneer work in this direction is presented in (Sørensen et al. 1996), where the problem of station-keeping and tracking for ships is addressed via Linear Quadratic Gaussian (LQG) control and a model reference feedforward controller. The dynamic positioning of a ship is also considered in (Pettersen and Nijmeijer 2001); the proposed time-varying control law provides semi-global practical asymptotic stability against environmental forces of unknown magnitude, but known direction. In (Aguiar and Pascoal 2007) the dynamic positioning of an underactuated AUV in the presence of a constant, unknown current is considered; an adaptive controller yields convergence to a desired target point, whereas the final orientation of the vehicle is aligned with the direction of the current. The same philosophy regarding the final orientation is adopted in (Pereira et al. 2008), which addresses the station-keeping for a surface vessel in the presence of wind disturbances. In (Aguiar et al. 2007) the authors propose a switching feedback control law which stabilizes an underactuated AUV around a small neighborhood of the origin, yielding input-to-state practical stability in the presence of disturbances and measurement noise. A hybrid control design for dynamic positioning from calm to extreme sea conditions is proposed in (Nguyen et al. 2007); this work utilizes a supervisory switching logic for orchestrating the switching among different candidate controllers that satisfy the structural changes in the hydrodynamics and the performance requirements subject to varying environmental conditions. Dynamic positioning has been also addressed using sliding-mode control in (Tannuri et al. 2010) and using fuzzy control in (Chang et al. 2002).

[1] A dynamic positioning control system typically consists of several submodules, including signal processing from sensors, wave filtering and state estimation, controller logic for different modes of operation, high-level feedback control laws, feedforward control laws, guidance system and reference trajectories, low-level thrust allocation and model adaptation in various operational and environmental conditions (Sørensen 2011).

Despite these contributions, it is generally accepted that the stabilization of underactuated underwater vehicles in the presence of disturbances has only been partially addressed and is still open in many respects (Aguiar et al. 2007).

1.2 *Problem Overview and Contributions*

Allowing the desired orientation of a marine vehicle to be essentially specified by external disturbances, as done in (Pettersen and Fossen 2000, Pettersen and Nijmeijer 2001, Aguiar and Pascoal 2007, Pereira et al. 2008), is a plausible assumption and often beneficial for many practical applications, for instance when a marine vehicle needs to move among predefined waypoints to accomplish a mission, or reach a specific spatial region. Yet, there may be cases where a marine vehicle should not only remain close to a desired position, but also to attain a desired (range of) orientation(s) as well. For instance, it is common practice to employ a relatively small, agile underwater robotic vehicle for the inspection of an underwater structure (e.g. oil platform, ship hull), a ship wreck, or marine population, via its onboard camera. In such cases, it may be desirable to keep both the position and the orientation of the vehicle close to nominal values, so that the inspection task (for instance, taking snapshots from a predefined set of configurations (positions and orientations) with respect to (w.r.t.) the target) is essentially effective.[1] Let us consider for instance a marine (underwater, surface) vehicle, which is used to inspect a stationary target through its onboard, non-rotating, camera (Fig. 1). The position and orien-

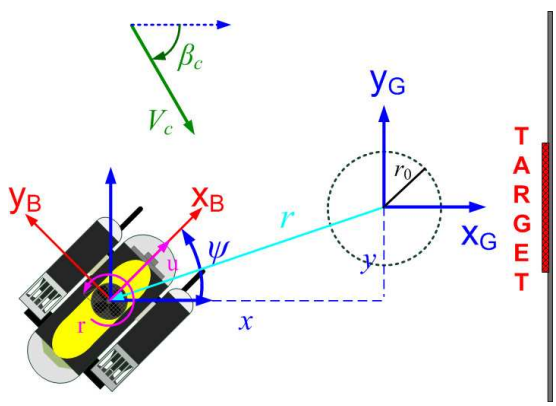

Figure 1. The considered scenario: The marine vehicle should be driven and remain into a neighborhood of the origin $\boldsymbol{q_G} = \mathbf{0}$, despite the effect of the current disturbance V_c, and while the direction β_c is not necessarily constant.

tation trajectories of the vehicle are ideally required to be asymptotically stable w.r.t. to the origin $\boldsymbol{q_G} = \mathbf{0}$, where $\boldsymbol{q} \in \mathbb{R}^2 \times \mathcal{S}$ denotes the pose (position and orientation) vector w.r.t. $\mathcal{G}$. However, the perturbation induced by the current disturbance of velocity V_c and direction β_c w.r.t. a global frame $\mathcal{G}$, is non-vanishing at $\boldsymbol{q_G}$ and thus the origin is not an equilibrium point. Consequently, it is meaningless to search for control laws that yield the system asymptotically stable at $\boldsymbol{q_G}$. Instead, one can aim at rendering the system uniformly ultimately bounded within a set that contains the origin, addressing thus the practical stabilization problem.

Motivated by these considerations, this paper proposes a switching control strategy and design which yields global, practical stability for an underactuated marine vehicle under the effect of unknown, but bounded, non-vanishing current perturbations. Under the proposed control scheme, the vehicle converges and remains into a goal set around the origin. The resulting performance is achieved via state-dependent switching among three state feedback controllers.

[1]Inspection could plausibly be facilitated by a rotating camera along the vertical axis (pan camera). In that case, the vehicle can be controlled to align with and counteract the current (external) disturbance, and the camera can be controlled to carry out the inspection task according to some predefined criteria; yet this assumption essentially defines a different control problem with the system having an extra degree-of-freedom (d.o.f.). Here we assume that the onboard camera can not rotate along the yaw d.o.f., which holds true for many low-cost commercial underwater robotic vehicles.

The first controller is active outside the goal set and drives the system trajectories into this set using a dipolar vector field (Panagou et al. 2011). The other two controllers are active inside the goal set, and alternately regulate either the position, or the orientation of the vehicle. The switched system is shown to be robust, in the sense that the system trajectories enter and remain into the goal set even when only a maximum bound $\|\boldsymbol{v}\|_{\max}$ on the current disturbance is given, while the direction of the current β_c is not necessarily constant.

Compared to earlier relevant work on dynamic positioning for underactuated marine vehicles, which drop the specification on the desired orientation, the proposed control strategy allows also for the regulation of the vehicle's orientation to zero during the time intervals when the corresponding controller is active. This feature, along with the robustness property, renders the proposed solution suitable for applications where *both the position and the orientation of an autonomous marine vehicle are of importance*, e.g. for inspection tasks with a fixed (i.e. non-rotating) onboard camera. Furthermore, our control strategy does not require the disturbance direction to be either constant, or a priori known, or estimated on-line, as done in (Pettersen and Nijmeijer 2001, Aguiar and Pascoal 2007); only the maximum bound on the disturbance magnitude is required to be known. Compared to other hybrid control solutions (Nguyen et al. 2007) for dynamic positioning, our strategy differs in the sense that it does not involve an orchestration among controllers for various environmental conditions, but is rather an orchestration among different state-dependent controllers which yield the position trajectories ultimately bounded around the origin, against a bounded class of disturbances. Finally, it should be mentioned that the proposed switching control logic has been in part inspired by the notion of "unstable/stable switched systems" in (Aguiar et al. 2007). However, the overall control design and analysis is not similar with those in (Aguiar et al. 2007), while the use of the dipolar vector fields renders the navigation and control design much more intuitive and straightforward, without the need for coordinate transformations, as done in (Aguiar et al. 2007).

Preliminary results of this work have appeared in (Panagou and Kyriakopoulos 2011), where the proposed control strategy is implemented for a vehicle with unicycle kinematics, subject to an unknown, but bounded, velocity disturbance. Compared to this paper, here the control design is based on the 3-d.o.f. equations for the motion of a marine vehicle, including both the kinematics and the vehicle dynamics; consequently, the control design and stability analysis are not the same with the ones in (Panagou and Kyriakopoulos 2011). Furthermore, the dipolar vector field used in this paper is of simpler analytic form compared to the one used in (Panagou and Kyriakopoulos 2011). Finally, more simulation results are included, which demonstrate the efficacy of the proposed switching control strategy in the case that the direction of the current disturbance is not constant, but subject to zero-mean, uniform deviation w.r.t. an unknown direction.

The paper is organized as follows: Section 2 gives the problem formulation and Section 3 briefly introduces the notion of dipolar vector fields used in the control design. Section 4 presents the switching control strategy, while the analytic construction of the control laws, the stability analysis of the switched system and the robustness consideration are given in Section 5. Section 6 includes the simulation results. The conclusions and thoughts on future research are summarized in Section 7.

2 Problem Formulation

We consider the motion on the horizontal plane of a marine vehicle which has two back thrusters for moving along the surge and yaw d.o.f., but no lateral thruster along the sway d.o.f.. The considered thrust allocation pattern is encountered on many commercial underwater and surface robotic vehicles, while it furthermore constitutes a standard configuration for many custom-made AUVs with reconfigurable thrust allocation. The roll angle ϕ and the pitch angle θ are assumed to be passively stable around zero, i.e. $\phi = \theta = 0$.

We assume that the vehicle moves under the influence of an non-rotational current of velocity

V_c and direction β_c w.r.t. a global cartesian coordinate frame $\mathcal{G}$. Following (Fossen 2002), the equations of motion along surge, sway and yaw d.o.f. are given as:

$$\dot{x} = u_r \cos\psi - v_r \sin\psi + V_c \cos\beta_c \tag{1a}$$

$$\dot{y} = u_r \sin\psi + v_r \cos\psi + V_c \sin\beta_c \tag{1b}$$

$$\dot{\psi} = r \tag{1c}$$

$$m_{11}\dot{u}_r = m_{22} v_r r + X_u u_r + X_{u|u|}\,|u_r|\,u_r + \tau_u \tag{1d}$$

$$m_{22}\dot{v}_r = -m_{11} u_r r + Y_v v_r + Y_{v|v|}\,|v_r|\,v_r \tag{1e}$$

$$m_{33}\dot{r} = (m_{11} - m_{22}) u_r v_r + N_r r + N_{r|r|}\,|r|\,r + \tau_r, \tag{1f}$$

where $\boldsymbol{q} = \left[\boldsymbol{r}^\top \;\; \psi\right]^\top = [x \;\; y \;\; \psi]^\top$ is the configuration (pose) vector w.r.t. the global frame $\mathcal{G}$, $\boldsymbol{r} = [x \;\; y]^\top$ is the position vector and ψ is the orientation (yaw angle) of the vehicle w.r.t. $\mathcal{G}$, and $\boldsymbol{\nu_r} = [u_r \;\; v_r \;\; r]^\top$ is the vector of relative (linear and angular) velocities w.r.t. the body-fixed frame $\mathcal{B}$, defined as: $\boldsymbol{\nu_r} = \boldsymbol{\nu} - \boldsymbol{\nu_c}$, where $\boldsymbol{\nu} = [u \;\; v \;\; r]^\top$ are the linear and angular velocities of the vehicle w.r.t. $\mathcal{B}$, and $\boldsymbol{\nu_c} = [V_c \cos(\beta_c - \psi) \;\; V_c \sin(\beta_c - \psi) \;\; 0]^\top$ are the current velocities w.r.t. $\mathcal{B}$. Furthermore: m_{11}, m_{22}, m_{33} are the terms of the inertia matrix including the added mass effect along the axes of $\mathcal{B}$,[1] X_u, Y_v, N_r are the linear drag terms, $X_{u|u|}$, $Y_{v|v|}$, $N_{r|r|}$ are the nonlinear drag terms, and τ_u, τ_r are the control inputs along the surge and yaw d.o.f..

Remark 2.1 The model (1) neglects the off-diagonal elements of the inertia and damping matrices, in the sense that they are relatively small compared to the dominating diagonal elements. This is considered a valid assumption for fully submerged vehicles which have three planes of symmetry and move at low speed in the presence of ocean currents (Fossen 2002), and furthermore has been used in earlier related work on dynamic positioning Aguiar et al. (2007), Aguiar and Pascoal (2007). Yet, the output feedback control design for an AUV of more complicated modeling, which includes off-diagonal inertia and linear damping elements that couple the sway and yaw d.o.f., has been addressed in Refsnes et al. (2007, 2008). Motivated in part by this, we furthermore illustrate the effectiveness of the proposed control design in the case of port-starboard symmetry only, i.e. for a model with off-diagonal elements in the inertia and damping matrices, see Section 6.

Remark 2.2 Note that the (in general destabilizing) yaw Munk moment N_{Munk} is included in the model (1) through equation (1f), since $(m_{11} - m_{22})u_r v_r = (m - X_{\dot{u}} - (m - Y_{\dot{v}}))u_r v_r = (Y_{\dot{v}} - X_{\dot{u}})u_r v_r = N_{Munk}$. In any case, one should keep in mind that the added mass inertia and coriolis matrices have been modeled in various ways in earlier work, depending on the assumptions mentioned above and the control objectives; for more details see Refsnes et al. (2007, 2008).

The system (1) falls into the class of control affine systems with drift vector field $\mathbf{f}(\mathbf{x})$ and additive perturbations $\boldsymbol{v}(\cdot)$, written as: $\dot{\mathbf{x}} = \mathbf{f}(\mathbf{x}) + \sum_{i=1}^{2} \mathbf{g}_i(\mathbf{x})\mathrm{u}_i + \boldsymbol{v}(\cdot)$, where $\mathbf{x} = \left[\boldsymbol{q}^\top \;\; \boldsymbol{\nu_r}^\top\right]^\top = [x \;\; y \;\; \psi \;\; u_r \;\; v_r \;\; r]^\top$ is the state vector, $\mathbf{g}_i(\cdot)$ are the control vector fields and $\boldsymbol{v}(\cdot) = [V_c \cos\beta_c \;\; V_c \sin\beta_c \;\; \mathbf{0}_{1\times 4}]^\top$ is the perturbation vector field. In the sequel, the perturbation vector field is denoted as $\boldsymbol{v}(\cdot) = [V_c \cos\beta_c \;\; V_c \sin\beta_c]^\top$.

The dynamics along the sway d.o.f. serves as a second-order nonholonomic constraint; the equation (1e) implies that $\mathbf{x_e} = \mathbf{0}$ is an equilibrium point of (1) if $v_r = 0$ and $u_r r = 0$. One gets out of the first condition that $v = v_c$. Given that the linear velocity v of the vehicle along the sway d.o.f. should be zero at the equilibrium, it follows that: $v_c = 0 \Rightarrow V_c \sin(\beta_c - \psi_e) = 0 \Rightarrow$

---

[1] To avoid ambiguity, let us note that m_{11}, m_{22}, m_{33} stand for the standard SNAME notation $m - X_{\dot{u}}$, $m - Y_{\dot{v}}$, $I - N_{\dot{r}}$, i.e. correspond to the inertia plus added mass matrix elements along surge, sway and yaw d.o.f. (Fossen 2002).

$V_c = 0$ or $\psi_e = \beta_c + \kappa\pi, \kappa \in \mathbb{Z}$. Thus, the desired orientation $\psi_e = 0$ can be an equilibrium of (1) if $V_c = 0$, which corresponds to the nominal case, or if $\beta_c = 0$, i.e. if the current is parallel to the x-axis of the global frame $\mathcal{G}$. In the general case that $\beta_c \neq 0$, the current serves as a non-vanishing perturbation at the (pose) equilibrium $\boldsymbol{q_e} = \mathbf{0}$, and therefore the closed-loop trajectories of (1) can only be rendered ultimately bounded in a neighborhood of $\boldsymbol{q_e}$. Thus, the control design for (1) reduces into addressing the *practical* stabilization problem, i.e. to find state feedback control laws so that the system trajectories $\boldsymbol{q}(t)$ remain bounded around the origin.

Problem Statement: *Given the system* (1)*, subject to current-induced perturbations* $\boldsymbol{v} = [V_c \cos\beta_c \;\; V_c \sin\beta_c]^\top$, $V_c > 0$, $\beta_c \in [0, 2\pi)$*, design a switching signal* $\sigma(\cdot) : \mathbb{R}^n \to \mathcal{I} = \{1, 2, \ldots, \chi\}$ *and* χ *feedback control laws* $\boldsymbol{\gamma}_\sigma(\cdot)$*, so that the closed-loop system is* ε*-practically asymptotically stable around the origin, in the sense that for given* $\varepsilon > 0$ *and any initial* $\boldsymbol{q}_0$ *the solution* $\boldsymbol{q}(t) = \boldsymbol{q}(t, \boldsymbol{q}_0, \boldsymbol{\gamma}_\sigma(\cdot))$ *exists* $\forall t \geq 0$*, and furthermore* $\boldsymbol{q}(t) \in \mathcal{B}(\mathbf{0}, \varepsilon)$*,* $\forall t \geq T$*, where* $T = T(\boldsymbol{q}_0) > 0$*.*

3 Dipolar Vector Fields

The control design employs in part the concept of dipolar vector fields (Panagou et al. 2011). In its simplest form, a dipolar vector field $\mathbf{F} : \mathbb{R}^2 \to \mathbb{R}^2$ is defined on a 2-dimensional vector space, has integral curves that all contain the origin $(0, 0)$ of the global coordinate frame, is non-vanishing everywhere in $\mathbb{R}^2$ except for the origin, and is given as:

$$\mathbf{F}(\boldsymbol{r}) = \lambda(\boldsymbol{p}^\top \boldsymbol{r})\boldsymbol{r} - \boldsymbol{p}(\boldsymbol{r}^\top \boldsymbol{r}), \tag{2}$$

where $\lambda \geq 2$, $\boldsymbol{p} = [p_x \;\; p_y]^\top$ and $\boldsymbol{r} = [x \;\; y]^\top$ is the vector of (position) coordinates w.r.t. the frame $\mathcal{G}$, see Fig. 2(a) the vector field for $\lambda = 2$, $\boldsymbol{p} = [1 \;\; 0]^\top$.

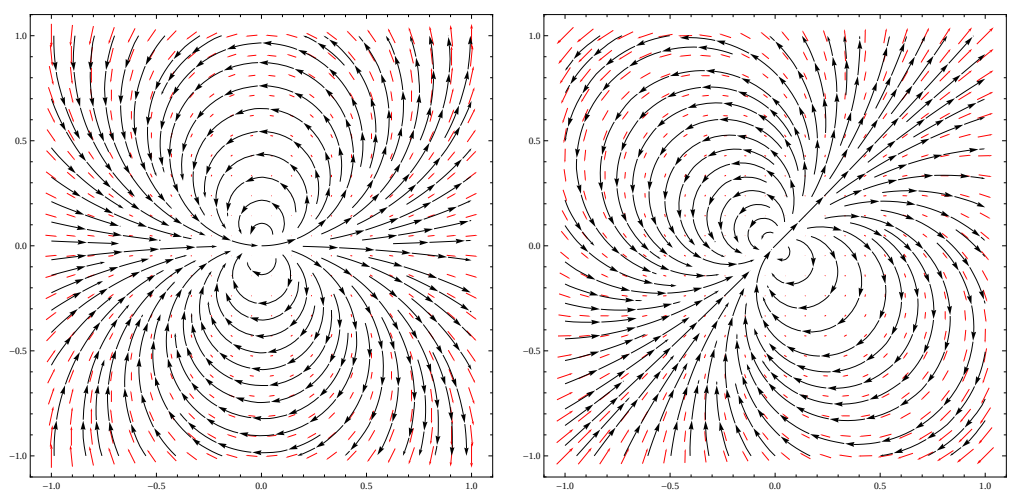

(a) The nominal field $\mathbf{F_n}$ (b) The perturbed field $\mathbf{F_p}$

Figure 2. The vector fields $\mathbf{F_n}(x, y)$ and $\mathbf{F_p}(x, y)$ for $\lambda = 2$, $\boldsymbol{p_n} = [1 \;\; 0]^\top$, $\boldsymbol{p_p} = [\cos\beta_c \;\; \sin\beta_c]^\top$. The integral curves converge to $(x, y) = (0, 0)$ with the direction $\phi_n = \text{atan2}(0, 1)$ and $\phi_p = \text{atan2}(\sin\beta_c, \cos\beta_c)$ of the vectors $\boldsymbol{p_n}$ and $\boldsymbol{p_p}$, respectively.

The main characteristic of a dipolar vector field (2) is that its integral curves converge to $(0, 0)$ with the direction $\phi_p = \text{atan2}(p_y, p_x)$ of the dipole moment vector $\boldsymbol{p}$. Consequently, choosing the vector $\boldsymbol{p}$ such that $\phi_p = \text{atan2}(p_y, p_x) \triangleq \psi_d$ reduces the problem of steering the vehicle to a desired configuration $\boldsymbol{q_d} = [0 \;\; 0 \;\; \psi_d]^\top$ into forcing the vehicle to align with and flow along the integral curves of the dipolar vector field $\mathbf{F}(\cdot)$. In other words, the 2-dimensional dipolar vector field $\mathbf{F}(\cdot)$ can serve as a feedback motion plan (LaValle 2006) for the system, since by

construction the integral curves offer reference paths to $(x, y) = (0, 0)$ which converge there with the desired orientation $\psi_d \triangleq \text{atan2}(p_y, p_x)$.

Following this idea, and assuming for now that the current velocity V_c and orientation β_c are known[1], one can easily construct a dipolar vector field $\mathbf{F_p}(\cdot)$ for the perturbed system (1), with integral curves converging to the equilibrium $\boldsymbol{q_e} = [x_e \;\; y_e \;\; \psi_e]^\top$ of (1). The vector field $\mathbf{F_p}(\cdot)$ is taken out of the family of dipolar vector fields (2), and is generated by a dipole moment vector $\boldsymbol{p_p} = [p_x \;\; p_y]^\top$ such that $\tan\psi_e = \tan\beta_c \triangleq \frac{p_y}{p_x}$.

Consequently, for $\boldsymbol{p_p} = [\cos\beta_c \;\; \sin\beta_c]^\top$ and $\lambda = 2$ one gets a dipolar vector field $\mathbf{F_p}(x, y) = \mathrm{F}_{px}\,\hat{\boldsymbol{x}} + \mathrm{F}_{py}\,\hat{\boldsymbol{y}}$ (Fig. 2(b)), where the analytic expressions of the vector field components F_{px}, F_{py} along the unit coordinate vectors are taken out of equation (2) and read:

$$\mathrm{F}_{px} = x^2\cos\beta_c + 2xy\sin\beta_c - y^2\cos\beta_c, \tag{3a}$$

$$\mathrm{F}_{py} = y^2\sin\beta_c + 2xy\cos\beta_c - x^2\sin\beta_c. \tag{3b}$$

4 Switching Control Strategy

Having the vector field $\mathbf{F_p}(x, y)$ given by (3) at hand now reduces the control design into finding a state feedback control law $\boldsymbol{\gamma}_1(\cdot)$ which forces the vehicle to follow the integral curves of (3) as reference paths. Let us denote the system (1) under the control law $\boldsymbol{\gamma}_1(\cdot)$ as the (closed-loop) system $\dot{\boldsymbol{q}} = \boldsymbol{f}_1(\boldsymbol{q}, \boldsymbol{\gamma}_1)$. Clearly, such a control law would cause the position $\boldsymbol{r} = [x \;\; y]^\top$ of the vehicle to converge to the origin $(x, y) = (0, 0)$, whereas the orientation ψ would converge to the orientation ϕ_p of the dipole moment vector $\boldsymbol{p_p} = [\cos\beta_c \;\; \sin\beta_c]^\top$. Inspired by (Aguiar et al. 2007), we say that the system $\boldsymbol{f}_1(\boldsymbol{q}, \boldsymbol{\gamma}_1)$ is stable w.r.t. the position $\boldsymbol{r}$ and unstable w.r.t. the orientation ψ, in the sense that ψ does not converge to the desired value $\psi_d = 0$.

In fact, since $\boldsymbol{q_G} = \mathbf{0}$ is not an equilibrium point of (1), it follows that forcing the orientation $\psi \to 0$ via a control law $\boldsymbol{\gamma}_2(\cdot)$ will result in a system $\dot{\boldsymbol{q}} = \boldsymbol{f}_2(\boldsymbol{q}, \boldsymbol{\gamma}_2)$ of stable orientation ψ, but unstable position $\boldsymbol{r}$. In other words, one needs to make a trade-off between regulating the position $\boldsymbol{r}$ to a desired value $\boldsymbol{r_d}$ and regulating the orientation ψ to a desired value ψ_d. In this sense, one may resort to a switching control strategy between the systems $\boldsymbol{f}_1(\boldsymbol{q}, \boldsymbol{\gamma}_1)$, $\boldsymbol{f}_2(\boldsymbol{q}, \boldsymbol{\gamma}_2)$, to alternately force either the position $\boldsymbol{r}$, or the orientation ψ to their desired values, to eventually get an ε-practically stable system.

To design a state-dependent switching control strategy, we first assume that the direction of the current disturbance is known, i.e. that the unit vector $\hat{\boldsymbol{v}} = [\cos\beta_c \;\; \sin\beta_c]^\top$ of the current velocities w.r.t. the global frame $\mathcal{G}$ is known.[2]

We then partition the configuration space $\mathcal{C} \subseteq \mathbb{R}^2 \times [0, 2\pi)$ into the operating regions K and G, such that $K = \{\boldsymbol{q} = \left[\boldsymbol{r}^\top \;\; \psi\right]^\top \in \mathcal{C} \mid \|\boldsymbol{r}\| > r_0\}$, for some $r_0 > 0$, and $G = \mathcal{C} \setminus K$ (Fig. 3(a)). The region K is further divided into $A = \{\boldsymbol{q} \in K \mid \langle \boldsymbol{r}, \hat{\boldsymbol{v}}\rangle \geq 0\}$ and $B = \{\boldsymbol{q} \in K \mid \langle \boldsymbol{r}, \hat{\boldsymbol{v}}\rangle < 0\}$, with $K = (A \cup B)$. The region G is similarly divided into $G_1 = \{\boldsymbol{q} \in G \mid \langle \boldsymbol{r}, \hat{\boldsymbol{v}}\rangle \geq 0\}$ and $G_2 = \{\boldsymbol{q} \in G \mid \langle \boldsymbol{r}, \hat{\boldsymbol{v}}\rangle < 0\}$, with $G = (G_1 \cup G_2)$. The division of the region G is inspired by the following consideration: When $\boldsymbol{q} \in G_1$, the disturbance $\boldsymbol{v}$ forces the position trajectories $\boldsymbol{r}(t)$ of the (uncontrolled) system (1) away from the desired value $(0, 0)$, whereas when $\boldsymbol{q} \in G_2$, the disturbance forces the position trajectories $\boldsymbol{r}(t)$ towards the desired value $(0, 0)$.

Given this state space partitioning, the main idea for the control design is now the following: If $\boldsymbol{q} \in K$, then a control law based on the dipolar vector field (3) drives the system trajectories into the set G. Then, while $\boldsymbol{q} \in G$, the system switches to a control law that regulates the orientation $\psi \to 0$. However, since the regulation of the orientation ψ may yield instability w.r.t. the position $\boldsymbol{r}$, it is preferable to control the orientation of the vehicle when the current

[1]The assumption on known direction β_c is later dropped in Section 5.3.
[2]This assumption is later dropped, in the sense that only the maximum bound of V_c is considered to be known.

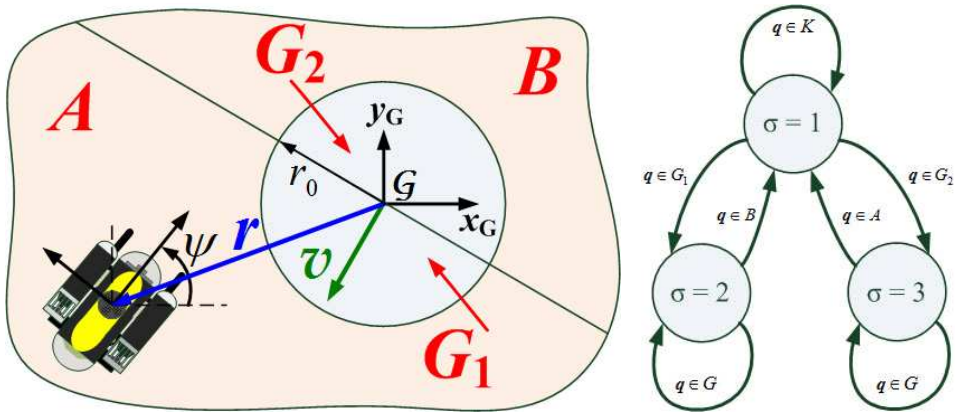

(a) The operating regions and system description w.r.t. frame $\mathcal{G}$.(b) The state-dependent switching logic.

Figure 3.

disturbance $\boldsymbol{v}$ forces the position of the vehicle towards the origin, i.e. when $\boldsymbol{q} \in G_2$. Therefore, if the system trajectories $\boldsymbol{q}(t)$ enter the set G_1 after leaving K, an additional control law is needed to drive $\boldsymbol{q}(t)$ into G_2. This consideration eventually results into switching among $\chi = 3$ candidate controllers $\boldsymbol{\gamma}_\sigma(\cdot)$, $\sigma \in \{1, 2, 3\}$. Briefly:

(1) If $\boldsymbol{q} \in K$, then the control law $\boldsymbol{\gamma}_1(\cdot)$ forces the position trajectories into G, yielding stable position $\boldsymbol{r}$ and unstable orientation ψ; in fact, the orientation ψ of the vehicle is forced to be stable to the orientation $\phi \triangleq \text{atan2}(\mathrm{F}_{py}, \mathrm{F}_{px})$ of the vector field $\mathbf{F_p}(x, y)$, i.e. $\psi \to \phi$.
(2) In the case that $\boldsymbol{r}$ reaches G_1 after leaving K, then the control law $\boldsymbol{\gamma}_2(\cdot)$ forces the position trajectories into the region B through the region G_2; thus, both $\boldsymbol{r}$ and ψ are rendered unstable, in the sense that $\|\boldsymbol{r}\| \to r_0$ and $\psi \to \phi_p$.
(3) In the case that $\boldsymbol{r}$ reaches G_2 after leaving K, or reaches B after leaving G_2, then the control law $\boldsymbol{\gamma}_3(\cdot)$ regulates the orientation $\psi \to 0$, yielding unstable $\boldsymbol{r}$ and stable ψ.

Consequently, the possible state (position) transitions are: $A \rightleftarrows G_1$, $G_1 \rightleftarrows G_2$, $G_2 \rightleftarrows B$. The above described control strategy can be implemented by the following hysteresis-based switching logic (Fig. 3(b)): If $\boldsymbol{q}(0) \in K$, then $\sigma(\boldsymbol{q}(0)) = 1$, else $\sigma(\boldsymbol{q}(0)) = 3$. For all $t > 0$,

- If $\boldsymbol{q}(t) \in K$ and $\sigma(\boldsymbol{q}(t^-)) = 1$, then $\sigma(\boldsymbol{q}(t)) = 1$.
- If $\boldsymbol{q}(t) \in G_1$ and $\sigma(\boldsymbol{q}(t^-)) = 1$, then $\sigma(\boldsymbol{q}(t)) = 2$.
- If $\boldsymbol{q}(t) \in G_2$ and $\sigma(\boldsymbol{q}(t^-)) = 1$, then $\sigma(\boldsymbol{q}(t)) = 3$.
- If $\boldsymbol{q}(t) \in G$ and $\sigma(\boldsymbol{q}(t^-)) = 2$, then $\sigma(\boldsymbol{q}(t)) = 2$.
- If $\boldsymbol{q}(t) \in B$ and $\sigma(\boldsymbol{q}(t^-)) = 2$, then $\sigma(\boldsymbol{q}(t)) = 3$.
- If $\boldsymbol{q}(t) \in B$ and $\sigma(\boldsymbol{q}(t^-)) = 3$, then $\sigma(\boldsymbol{q}(t)) = 3$.
- If $\boldsymbol{q}(t) \in G$ and $\sigma(\boldsymbol{q}(t^-)) = 3$, then $\sigma(\boldsymbol{q}(t)) = 3$.
- If $\boldsymbol{q}(t) \in A$ and $\sigma(\boldsymbol{q}(t^-)) = 3$, then $\sigma(\boldsymbol{q}(t)) = 1$.

Note that hysteresis into the design of the state-dependent switching signal $\sigma(\boldsymbol{q}(t))$ is introduced by taking into account both the current value of $\boldsymbol{q}(t)$ and the previous value of the switching signal $\sigma(\boldsymbol{q}(t^-))$. Thus, the hysteresis-based switching logic: (i) results in a hybrid closed-loop control system with σ being the discrete state, since the value of σ is not determined by the current value of $\boldsymbol{q}(t)$ alone, but is also depended on its previous value, $\sigma = \varphi(\boldsymbol{q}, \sigma^-)$, and (ii) prevents the appearance of chattering when the state crosses the switching surfaces (Liberzon 2003).

5 Control Design

Having the switching strategy at hand, we now need to design the candidate state feedback controllers $\boldsymbol{\gamma}_\sigma(\cdot)$, $\sigma \in \{1,2,3\}$ that regulate either the position, or the orientation of the marine vehicle. Following common practice for this class of systems, the system (1) is divided into two subsystems Σ_1, Σ_2, where Σ_1 consists of the kinematic equations (1a)-(1c) and the sway dynamics (1e), while the dynamic equations (1d), (1f) constitute the subsystem Σ_2.

The velocities $[u_r \;\; r]^\top$ are considered as virtual control inputs for the subsystem Σ_1, while the actual control inputs $\boldsymbol{\tau} = [\tau_u \;\; \tau_r]^\top$ are used to control the subsystem Σ_2. Thus, the problem reduces into: first, designing the virtual control inputs $\boldsymbol{\gamma}_\sigma(\cdot)$ for the subsystem Σ_1, and second, ensuring that the actual velocity trajectories of subsystem Σ_2 are asymptotically stable to the virtual velocity inputs $\boldsymbol{\gamma}_\sigma(\cdot)$, by suitably defining the control inputs $\boldsymbol{\tau}$.

5.1 *Control design at the kinematic level*

5.1.1 Design of the control law $\boldsymbol{\gamma}_1(\cdot)$

The control law $\boldsymbol{\gamma}_1(\cdot)$ forces the system to align with the vector field (3) while converging to the desired position $(0,0)$. Let us denote with $\boldsymbol{p_p} \triangleq \boldsymbol{p} = [p_x \;\; p_y]^\top$ the dipole moment vector which generates the vector field (3). Note also that we would like the direction $\phi_p = \operatorname{atan2}(p_y, p_x)$ of the integral curves at $(0,0)$ to lie in the interval $\left[-\frac{\pi}{2}, \frac{\pi}{2}\right]$, so that the vehicle faces a target of interest as shown in Fig. 1. Thus, we need a vector $\boldsymbol{p}$ such that $\boldsymbol{p}^\top \hat{\boldsymbol{x}}_{\mathcal{G}} > 0 \Rightarrow p_x > 0$. Therefore, we take $\boldsymbol{p} \triangleq \operatorname{sgn}(\cos\beta_c)\,[\cos\beta_c \;\; \sin\beta_c]^\top$, which implies that if $\cos\beta_c \geq 0$, then $\boldsymbol{p} \triangleq \hat{\boldsymbol{v}}$, whereas if $\cos\beta_c < 0$, then $\boldsymbol{p} \triangleq -\hat{\boldsymbol{v}}$.

Theorem 5.1 The position trajectories $\boldsymbol{r}(t) = [x(t) \;\; y(t)]^\top$ of the system (1) enter a ball $\mathcal{B}(\mathbf{0}, r_0)$ for any $\boldsymbol{r}(0) \notin \mathcal{B}(\mathbf{0}, r_0)$, under the control law $\boldsymbol{\gamma}_1(\cdot)$ given as:

$$u_{r,d} = -k_1 \operatorname{sgn}\left(\boldsymbol{r}^\top \begin{bmatrix} \cos\psi \\ \sin\psi \end{bmatrix}\right) \|\boldsymbol{r}\| - \operatorname{sgn}(\boldsymbol{p}^\top \boldsymbol{r}) \|\boldsymbol{v}\|, \tag{4a}$$

$$r_d = -k_2(\psi - \phi), \tag{4b}$$

where $k_1, k_2 > 0$, $\phi = \operatorname{atan2}(\mathrm{F}_{py}, \mathrm{F}_{px})$ is the orientation of the vector field (3) at (x,y), and the function $\operatorname{sgn}(\cdot)$ is defined as $\operatorname{sgn}(a) = \begin{cases} 1, & \text{if } a \geq 0, \\ -1, & \text{if } a < 0, \end{cases}$

The proof is given in Appendix A.

5.1.2 Design of the control laws $\boldsymbol{\gamma}_2(\cdot)$ and $\boldsymbol{\gamma}_3(\cdot)$

Let us denote with ∂X_Y the boundary of a set X w.r.t. a neighbor set Y. Theorem 5.1 guarantees that, under the control law (4), the configuration (pose) trajectories $\boldsymbol{q}(t)$ of the system enter the set $G = \{\boldsymbol{q} = \left[\boldsymbol{r}^\top \;\; \psi\right]^\top \in \mathcal{B}(\mathbf{0}, r_0) \times [0, 2\pi)\}$. Once the system has entered the set G, let us consider the following two cases:

(1) Assume that $\boldsymbol{q} \in G_1 = \{G \mid \langle \boldsymbol{r}, \boldsymbol{v} \rangle \geq 0\}$, i.e. that the system trajectories $\boldsymbol{q}(t)$ have entered the set G_1. In this set, the current disturbance $\boldsymbol{v}$ forces the vehicle away from the origin $(x,y) = (0,0)$. Then:

Theorem 5.2 The system trajectories $\boldsymbol{q}(t)$ enter the set B under the control law $\boldsymbol{\gamma}_2(\cdot)$ given as:

$$u_{r,d} = -k_3 \operatorname{sgn}(\cos\beta_c) \|\boldsymbol{v}\|, \tag{5a}$$

$$r_d = -k_4(\psi - \phi_p), \tag{5b}$$

with $k_3 > 1$, $k_4 > 0$.

The proof is given in Appendix B.

(2) Assume that $\boldsymbol{q} \in G_2 = \{G \mid \langle \boldsymbol{r}, \boldsymbol{v} \rangle < 0\}$, i.e. that the system trajectories $\boldsymbol{q}(t)$ have entered the set G_2. In this set, the current disturbance $\boldsymbol{v}$ forces the vehicle towards the origin $(x, y) = (0, 0)$. Then:

Theorem 5.3 The position trajectories $\boldsymbol{r}(t)$ enter the set A under the control law $\boldsymbol{\gamma}_3(\cdot)$ given as:

$$u_{r,d} = 0, \quad r_d = -k_5 \psi, \quad k_5 > 0. \tag{6}$$

The proof is given in Appendix C.

5.1.3 *Stability of the switched system $\dot{\boldsymbol{q}} = \boldsymbol{f}_\sigma(\boldsymbol{q}, \boldsymbol{\gamma}_\sigma)$*

For analyzing the stability of the proposed state-dependent switching, we take into account that the properties of each subsystem $\boldsymbol{f}_\sigma(\boldsymbol{q}, \boldsymbol{\gamma}_\sigma)$ are of concern only in the regions where this system is active. Following (Branicky 1998), let us consider a strictly increasing sequence of times

$$\mathrm{T} = \{t_0, t_1, \ldots, t_n, \ldots, \},$$

the interval completion $\mathrm{I}(\mathrm{T}) = \bigcup_{n \in \mathbb{N}} [t_{2n}, t_{2n+1}]$ of T, and the switching sequence

$$\Sigma = \{\boldsymbol{q}_0; (\iota_0, t_0), (\iota_1, t_1), \ldots, (\iota_n, t_n), \ldots \mid \iota_n \in \mathcal{I}, n \in \mathbb{N}\},$$

where t_0 is the initial time, $\boldsymbol{q}_0$ is the initial state and $\mathbb{N}$ is the set of nonnegative integers.

For $t \in [t_k, t_{k+1})$, one has $\sigma(t) = \iota_k$, that is the ι_k-th subsystem is active. For any $j \in \mathcal{I}$, let us denote with $\Sigma \mid j = \{t_{j_1}, t_{j_1+1}, t_{j_2}, t_{j_2+1}, \ldots, t_{j_\nu}, t_{j_\nu+1}, \ldots\}$ the sequence of switching times when the j-th subsystem is "switched on" or "switched off", with $\mathrm{E} \mid j = \{t_{j_1}, t_{j_2}, \ldots, t_{j_\nu}, \ldots\}$ being the "switched on" times of the j-th subsystem.

Theorem 5.4 (Zhao and Hill 2008, Thm 3.9) Assume that for each $j \in \mathcal{I}$, there exists a positive definite generalized Lyapunov-like function[1] $V_j(\boldsymbol{x})$ with respect to $\boldsymbol{f}_j(\boldsymbol{x}, 0)$ and the associated trajectory $\boldsymbol{x}(t)$. Then the origin of the system $\dot{\boldsymbol{x}} = \boldsymbol{f}_\sigma(\boldsymbol{x}, \boldsymbol{u}_\sigma)$, with $\boldsymbol{u}_\sigma \equiv 0$, is stable if and only if there exist class $\mathcal{GK}$[2] functions α_j satisfying

$$V_j\left(\boldsymbol{x}(t_{j_{k+1}})\right) - V_j\left(\boldsymbol{x}(t_{j_1})\right) \leq \alpha_j(\|\boldsymbol{x}_0\|), \quad k \geq 1, \quad j = 1, 2, \ldots, \chi. \tag{7}$$

This theorem states that stability is ensured as long as $V_j\left(\boldsymbol{x}(t_{j_{k+1}})\right) - V_j\left(\boldsymbol{x}(t_{j_1})\right)$, i.e. the change of V_j between any "switched on" time $t_{j_{k+1}}$ and the first active time t_{j_1}, is bounded by a class $\mathcal{GK}$ function, regardless of the initial value $V_j\left(\boldsymbol{q}(t_{j_1})\right)$ at the first active time.

Lemma 5.5 The position trajectories $\boldsymbol{r}(t)$ of the switched system $\dot{\boldsymbol{q}} = \boldsymbol{f}_\sigma(\boldsymbol{q}, \boldsymbol{\gamma}_\sigma)$, where $\sigma \in \mathcal{I} = \{1, 2, 3\}$, under the proposed switching logic, is Lyapunov stable.

Proof The correctness of the proposed lemma can be verified by a direct application of Theorem 5.4. Note that the initial condition $\boldsymbol{r}(0)$ may either be in K or in G, and that all the switchings occur when the state $\boldsymbol{q}$ crosses the switching surface $\mathcal{S} : \|\boldsymbol{r}\| = r_0$.

---

[1] A continuous function $V : \mathbb{R}^n \to [0, \infty)$ is called a generalized Lyapunov-like function for the vector field $\boldsymbol{f}$ and the associated trajectory $\boldsymbol{x}(t)$ over a strictly increasing sequence of times T, if there exists a continuous function $\phi : [0, \infty) \to [0, \infty)$ with $\phi(0) = 0$, such that $V(\boldsymbol{x}(t)) \leq \phi(V(\boldsymbol{x}(t_{2n})))$, for all $t \in (t_{2n}, t_{2n+1})$ and all $n \in \mathbb{N}$ (Zhao and Hill 2008)

[2] A function $a : [0, \infty) \to [0, \infty)$ is called a class $\mathcal{GK}$ function if it is increasing and right continuous at the origin with $a(0) = 0$ (Zhao and Hill 2008)

For each subsystem $\sigma \in \{1, 2, 3\}$, consider the generalized Lyapunov-like function $V_\sigma(\boldsymbol{r}) = \|\boldsymbol{r}\|$. Note that V_σ serves as a generalized Lyapunov-like function even when $\sigma = 2$ or $\sigma = 3$ is the active subsystem, i.e. when $\boldsymbol{r}(t) \in G$, since its value is bounded in the sense that $V_\sigma(\boldsymbol{r}(t)) \leq \phi\left(V_\sigma(\boldsymbol{r}(t_k))\right) = \phi(r_0)$, where $t \in [t_k, t_{k+1})$ and $\phi(\cdot) = \|\boldsymbol{r}\|$.

At any "switched on" time instant $t_{\sigma n}$ with $n > 1$, (that is, for any "switched on" time instant after the first switch has occurred at $t_{\sigma 1}$), one has that $V_\sigma(\boldsymbol{r}(t_{\sigma n})) \leq r_\sigma$, where $r_\sigma = r_0 + \delta$ and $\delta > 0$ can be chosen arbitrarily small. Then, for any first active time $t_{\sigma 1}$, where clearly $V_\sigma(\boldsymbol{r}(t_{\sigma 1})) \geq 0$, one has $V_\sigma(\boldsymbol{r}(t_{\sigma n})) - V_\sigma(\boldsymbol{r}(t_{\sigma 1})) \leq r_\sigma$, that is, any growth of each V_σ is always bounded. □

In summary, the proposed switching control strategy guarantees that the trajectories $\boldsymbol{r}(t)$ of the perturbed system (1) are ε-practically asymptotically stable around the origin, in the sense that $\boldsymbol{r}(t)$ converges into a ball $\mathcal{B}(\mathbf{0}, \varepsilon)$, where $\varepsilon = r_0 + \delta$ and $\delta > 0$ can be made arbitrarily small, and remains into the ball for $t > T$, whereas the orientation ψ is regulated to zero during the time intervals that the subsystem $\boldsymbol{f}_3(\boldsymbol{q}, \boldsymbol{\gamma}_3)$ is active.

5.2 *Control design at the dynamic level*

Finally, the control inputs τ_u, τ_r of the subsystem Σ_2 should be designed so that the actual velocities $u_r(t)$, $r(t)$ are globally exponentially stable (GES) to the virtual control inputs $u_{r,d}(\cdot)$, $r_d(\cdot)$, for each $\boldsymbol{\gamma}_\sigma(\cdot)$.

Theorem 5.6 The actual velocities $u_r(t)$, $r(t)$ are GES to the virtual control inputs $u_{r,d}(\cdot)$, $r_d(\cdot)$, respectively, under the control laws $\tau_u = \xi_1(\cdot)$, $\tau_r = \xi_2(\cdot)$ given as:

$$\tau_u = m_{11}\alpha - m_{22}v_r r - X_u u_r - X_{u|u|}|u_r|u_r, \tag{8a}$$

$$\tau_r = m_{33}\beta - (m_{11} - m_{22})u_r r - N_r r - N_{r|r|}|r|r, \tag{8b}$$

where

$$\alpha = -k_u(u_r - u_{r,d}(\cdot)) + (\nabla u_{r,d}(\cdot))\dot{\boldsymbol{q}}, \quad k_u > 0, \tag{9a}$$

$$\beta = -k_r(r - r_d(\cdot)) + (\nabla r_d(\cdot))\dot{\boldsymbol{q}}, \quad k_r > 0, \tag{9b}$$

and $\nabla u_{r,d} = \begin{bmatrix} \frac{\partial u_{r,d}}{\partial x} & \frac{\partial u_{r,d}}{\partial y} & \frac{u_{r,d}}{\partial \psi} \end{bmatrix}$, $\nabla r_d = \begin{bmatrix} \frac{\partial r_d}{\partial x} & \frac{\partial r_d}{\partial y} & \frac{r_d}{\partial \psi} \end{bmatrix}$ the gradient of $u_{r,d}(\cdot)$ and $r_d(\cdot)$. The proof is given in the Appendix D.

5.3 *Robustness consideration*

The control design and stability analysis has been based on the assumption that the current $\boldsymbol{v} = [V_c \cos\beta_c \;\; V_c \sin\beta_c]^\top$ is known. However, this is quite unrealistic in general, since on-line measurements of the current velocity can not be easily acquired. An estimation of the current velocity is usually obtained using nonlinear observers, see for example in (Aguiar and Pascoal 2007, Refsnes et al. 2007), and then employed into the control design. However, this approach complicates the design and analysis of the overall closed-loop system, since both the estimation error and the state vector are required to be stable at zero. Therefore, guaranteeing the robustness of the switched system in the case that the current disturbance is unknown is meaningful for the class of problems considered here. Robustness reduces into guaranteeing that the system trajectories enter and remain into a ball $\mathcal{B}(\mathbf{0}, \varepsilon)$ of the origin.

To this end, let us assume that only a maximum bound $\|\boldsymbol{v}\|_{\max}$ on the disturbance is known, i.e. that $\|\boldsymbol{v}\| = \sqrt{(V_c \cos\beta_c)^2 + (V_c \sin\beta_c)^2} = V_c \leq \|\boldsymbol{v}\|_{\max}$, while the current direction $\beta_c = \operatorname{atan2}(\sin\beta_c, \cos\beta_c)$ is unknown, *and not necessarily constant*. In this case the vector $\boldsymbol{p}$ which

generates the vector field $\mathbf{F_p}(\cdot)$ can not be a priori determined, nor the proposed switching control strategy can be straightforward applied, since the term $\text{sgn}(\cos\beta_c)$ is unknown.

Thus, we consider the nominal vector field $\mathbf{F_n}$ out of (2) (see Fig. 2(a)), which is generated by a dipole moment vector $\boldsymbol{p_n} = [p \;\; 0]^\top$, where $p > 0$. For $p = 1$ and $\lambda = 2$ the vector field components F_{nx}, F_{ny} of $\mathbf{F_n} = \mathrm{F}_{nx}\,\hat{\boldsymbol{x}} + \mathrm{F}_{ny}\,\hat{\boldsymbol{y}}$ read:

$$\mathrm{F}_{nx} = x^2 - y^2, \tag{10a}$$

$$\mathrm{F}_{ny} = 2xy, \tag{10b}$$

while $\|\mathbf{F}\| = \sqrt{{\mathrm{F}_{nx}}^2 + {\mathrm{F}_{nx}}^2} \overset{(10)}{=} x^2 + y^2$. Consequently, regarding the control law $\boldsymbol{\gamma}_1(\cdot)$, one can verify that by following the same analysis as in Section 5.1.1, still gets the four cases in terms of $\text{sgn}(\boldsymbol{r}^\top\boldsymbol{v})$ and $\text{sgn}(\boldsymbol{p}^\top\boldsymbol{r})$, which effectively means that the system trajectories enter $\mathcal{B}(\mathbf{0}, r_0)$. In other words, the position trajectories $\boldsymbol{r}(t)$ of the vehicle robustly converge into $\mathcal{B}(\mathbf{0}, r_0)$ under any current disturbance $\boldsymbol{v}$ such that $\|\boldsymbol{v}\| \leq \|\boldsymbol{v}\|_{\max}$.

Similarly, the control laws (5), (6) while in $G = \{\boldsymbol{q} \in \mathcal{B}(\mathbf{0}, r_0) \times [0, 2\pi)\}$ can not be directly applied, since they depend on both $\text{sgn}(\boldsymbol{r}^\top\boldsymbol{v})$ and $\text{sgn}(\cos\beta_c)$. Nevertheless, the same idea on the switching control strategy can be used, where now the region G is divided into the region $G_1 = \{\boldsymbol{q} \in G \mid \langle \boldsymbol{p}, \boldsymbol{r}\rangle \leq 0\}$ and the region $G_2 = \{\boldsymbol{q} \in G \mid \langle \boldsymbol{p}, \boldsymbol{r}\rangle > 0\}$, with $G = (G_1 \cup G_2)$. Then, we have the following cases:

(1) if the vehicle reaches G_1 after leaving K, it is controlled so that it reaches B through G_2; this is achieved via the control law $\boldsymbol{\gamma}_2(\cdot)$ given as:

$$u_r = k_3\|\boldsymbol{v}\|, \tag{11a}$$

$$r = -k_4\psi. \tag{11b}$$

(2) if the vehicle reaches G_2 after leaving K, it is controlled so that it reaches A through G_1; this is achieved via the control law $\boldsymbol{\gamma}_3(\cdot)$ given as:

$$u_r = -k_3\|\boldsymbol{v}\|, \tag{12a}$$

$$r = -k_4\psi. \tag{12b}$$

In both cases, a gain $k_3 > 1$ on the linear velocity u_r is needed to counteract the destabilizing effect of the unknown lateral velocity induced by the current. At any case, the control law $\boldsymbol{\gamma}_1(\cdot)$ guarantees that the vehicle always re-enters into the region G.

6 Simulation Results

The efficacy of the switching control strategy is illustrated via simulations. We consider an under-actuated marine vehicle moving on the horizontal plane under the influence of an environmental disturbance $\boldsymbol{v} = [V_c\cos\beta_c \;\; V_c\sin\beta_c]^\top$. The dynamic (inertia, added mass, damping) parameters of (1) have been taken out of (Wang and Clark 2006) and are depicted in the table below in SI units. The goal configuration $\boldsymbol{q_G}$ is the origin $[0 \;\; 0 \;\; 0]^\top$, while the black line centered at $(0.5, 0)$

$m_{11} = m - X_{\dot{u}}$	5.5404	X_u	-2.3015	$X_{u\|u\|}$	-8.2845
$m_{22} = m - Y_{\dot{v}}$	9.6572	Y_v	-8.0149	$Y_{v\|v\|}$	-23.689
$m_{33} = I - N_{\dot{r}}$	0.0574	N_r	-0.0048	$N_{r\|r\|}$	-0.0089

is a point of interest, e.g. a target that the vehicle has to inspect through an onboard camera,

see Fig. 4(b) - 7(b).

In the scenarios throughout Fig. 4 - 6, the current disturbance $\boldsymbol{v}$ is assumed to be known, where $V_c = 0.1$ m/sec, and $\beta_c = -30,\ 30,\ 160$ deg, respectively. In Fig. 7 the current of velocity $V_c = 0.1$ m/sec and direction $\beta_c = 160$ deg is assumed to be unknown; the only information which is available to the switching controller is the bound $\|\boldsymbol{v}\|_{\max} = 0.1$. In all cases, the trajectories $x(t)$, $y(t)$ converge into the $\mathcal{B}(\mathbf{0}, r_0)$, where $r_0 = 0.15$ m, and remain bounded into the ball $\mathcal{B}(\mathbf{0}, \varepsilon)$, where $\varepsilon = r_0 + r_\varepsilon$, with r_ε being a small positive number,[1] see Fig. 4(b), 4(c) and Fig. 7(b), 7(c). The evolution of the system trajectories $\mathbf{x}(t)$ is depicted in Fig. 4(a), 7(a).

It is worth noting that the main difference between the scenarios in Fig. 6, where the current direction $\beta_c = 160$ deg is known, and Fig. 7, where the current direction $\beta_c = 160$ deg is unknown, lies in the evolution of the orientation trajectories $\psi(t)$. In particular, in the former case and while in region G, the orientation ψ is alternately regulated between zero (when the control law $\boldsymbol{\gamma}_3(\cdot)$ is active) and the direction ϕ_p of the vector $\boldsymbol{p}$ (when the control law $\boldsymbol{\gamma}_2(\cdot)$ is active). In the latter case, the orientation ψ is regulated to zero when the vehicle is in G, but oscillates with higher frequency. This behavior is due to the fact that the system switches more frequently between the control laws $\boldsymbol{\gamma}_1(\cdot)$, $\boldsymbol{\gamma}_2(\cdot)$ and $\boldsymbol{\gamma}_3(\cdot)$, since the destabilizing effect of the current-induced motion along the unactuated d.o.f. drives the vehicle faster out of the set G, compared to the first case. Still, the hysteresis-based switching among the controllers (4), (11), (12) prevents the appearance of chattering when crossing the switching surface.[2]

In Fig. 8 the system is subject to unknown current direction $\beta_c = 90$ deg, i.e. to a current perturbation that is vertical to the desired final orientation $\psi_d = 0$ and along the unactuated d.o.f. at this point. The system response and the resulting path demonstrate that the position trajectories remain bounded around the origin, while the switching among the candidate control laws is, as expected, much faster compared to the case in Fig. 7.

The proposed switching control strategy applies also in cases that the current direction β_c is not constant. In the scenario depicted in Fig. 9 the current direction is subject to zero-mean, uniform random deviation from the (unknown) nominal value β_c. Fig. 9(b) illustrates the path followed by the vehicle, while Fig. 9(c) demonstrates that the position trajectories remain bounded in the ball $\mathcal{B}(\mathbf{0}, \varepsilon)$.

Finally, the efficacy of the proposed control algorithm is demonstrated in the case of a vehicle with port-starboard symmetry only, i.e. when the system modeling includes off-diagonal elements in the inertia and linear damping matrices. More specifically, we consider the model of a surface vehicle (Fossen 2002) which includes the coupling between sway and yaw d.o.f. via the inertia (added mass) term $m_{23} = m_{32} = -Y_{\dot{r}} = 0.3943$ and the linear damping terms $Y_r = -4.0075$, $N_v = -6.6667 \times 10^{-4}$. The system response is given in Fig. 10. As expected, the vehicle's motion and resulting path (Fig. 10(b)) exposes a much more oscillatory behavior, compared to the previous cases, mostly due to the inertia term m_{23} which affects the underactuated (sway) d.o.f.. Yet, the main objective of the control design is fulfilled, since the position trajectories remain bounded in $\mathcal{B}(\mathbf{0}, \varepsilon)$, as demonstrated in 10(b), while the orientation $\psi(t)$ is regulated to zero during some time intervals, as demonstrated in Fig. 10(a).

7 Conclusions

This paper presented a switching control approach for the practical stabilization of an underactuated marine vehicle under non-vanishing, current-induced perturbations. The proposed control scheme is a hysteresis-based switching logic among three state feedback control laws. The first

[1]The size of the parameter r_ε depends on the inertia forces and moments in subsystem Σ_2. The faster the actual virtual velocities $u_r(t)$, $r_(t)$ converge to the virtual desired values $u_{r,d}$, r_d, then the faster the dynamic system (1) behaves as the "virtual" closed-loop kinematic subsystem Σ_1, and therefore in this case r_ε can be made arbitrarily small, $r_\varepsilon \to 0$.

[2]In the case of unknown current disturbances we assume that the (actual) relative linear velocities $u_r \triangleq u - V_c \cos(\beta_c - \psi)$, $v_r \triangleq v - V_c \sin(\beta_c - \psi)$ are not online available, but rather that only the body-fixed velocities u, v can be measured. Thus, instead of u_r, v_r in (8) we use the "worst-case relative velocities" $|u + V_c|$, $|v + V_c|$, respectively.

control law employs a dipolar vector field and drives the system trajectories into a set G around the origin. The other two control laws are active in G; switching between them renders the position of the vehicle practically stable, while the orientation is regulated to zero during some time intervals. The switched system is robust, in the sense that the system trajectories converge and remain into the set G even if only a bound $\|\boldsymbol{v}\|_{\max}$ on the current velocity is given. The proposed control approach is suitable for applications where both the position and the orientation of an underactuated vehicle is of importance, for instance in pursuing the dynamic positioning for a marine vehicle while inspecting a target of interest. Simulation results illustrate the efficacy of the approach. Future work can be towards the consideration of model parametric uncertainty as well as of more challenging perturbation models.

References

Aguiar, A.P., and Pascoal, A.M. (2001), "Regulation of a Nonholonomic Autonomous Underwater Vehicle with Parametric Modeling Uncertainty using Lyapunov Functions," in *Proc. of the 40th IEEE Conf. on Decision and Control*, Dec., Orlando, FL, USA, pp. 4178–4183.

Aguiar, A.P., and Pascoal, A.M. (2002), "Global stabilization of an underactuated autonomous underwater vehicle via logic-based switching," in *Proc. of the 41st IEEE Conf. on Decision and Control*, Dec., Las Vegas, NE, USA, pp. 3267–3272.

Aguiar, A.P., Hespanha, J.P., and Pascoal, A.M. (2007), "Switched seesaw control for the stabilization of underactuated vehicles," *Automatica*, 43, 1997–2008.

Aguiar, A.P., and Pascoal, A.M. (2007), "Dynamic positioning and way-point tracking of underactuated AUVs in the presence of ocean currents," *International Journal of Control*, 80, 1092–1108.

Branicky, M.S. (1998), "Multiple Lyapunov Functions and Other Analysis Tools for Switched and Hybrid Systems," *IEEE Transactions on Automatic Control*, 43, 475–482.

Brockett, R.W. (1983), "Asymptotic Stability and Feedback Stabilization," in *Differential Geometric Control Theory* eds. R. Brockett, R. Millman and H. Sussmann, Boston: Birkhauser, pp. 181–191.

Chang, W.J., Chen, G.J., and Yeh, Y.L. (2002), "Fuzzy Control of Dynamic Positioning Systems for Ships," *Journal of Marine Science and Technology*, 10, 47–53.

Cheng, J., Yi, J., and Zhao, D. (2002), "Stabilization of an Underactuated Surface Vessel via Discontinuous Control," in *Proc. of the 2007 American Control Conf.*, Jul., NY City, NY, USA, pp. 206–211.

Do, K.D., Jiang, Z.P., Pan, J., and Nijmeijer, H. (2002), "Global output feedback universal controller for the stabilization and tracking of underactuated ODIN-an underwater vehicle," in *Proc. of the 41st IEEE Conf. on Decision and Control*, Dec., Las Vegas, NE, USA, pp. 504–509.

Dong, W., and Guo, Y. (2005), "Global Time-Varying Stabilization of Underactuated Surface Vessel," *IEEE Trans. on Automatic Control*, 50, 859–864.

Fantoni, I., Lozano, R., Mazenc, F., and Pettersen, K.Y. (2000), "Stabilization of a nonlinear underactuated hovercraft," *Int. Journal of Robust and Nonlinear Control*, 10, 645–654.

Fossen, T.I., *Marine Control Systems: Guidance, Navigation and Control of Ships, Rigs and Underwater Vehicles*, Marine Cybernetics (2002).

Ghommam, J., Mnif, F., Benali, A., and Derbel, N. (2006), "Asymptotic Backstepping Stabilization of an Underactuated Surface Vessel," *IEEE Trans. on Control Systems Technology*, 14, 1150–1157.

Greytak, M., and Hover, F. (2008), "Underactuated Point Stabilization Using Predictive Models with Application to Marine Vehicles," in *Proc. of the 2008 IEEE/RSJ Int. Conf. on Intelligent Robots and Systems*, Sep., Nice, France, pp. 3756–3761.

Khalil, H.K., *Nonlinear Systems. Third Edition*, Prentice-Hall Inc. (2002).

Kim, T., Basar, T., and Ha, I.J. (2002), "Asymptotic Stabilization of an Underactuated Sur-

face Vessel via Logic-Based Control," in *Proc. of the 2002 American Control Conf.*, May, Anchorage, AL, USA, pp. 4678–4683.

LaValle, S.M., *Planning Algorithms*, Cambridge University Press (2006).

Liberzon, D., *Switching in Systems and Control*, Birkhauser Boston (2003).

Ma, B. (2009), "Global κ-exponential asymptotic stabilization of underactuated surface vessels," *Systems and Control Letters*, 58, 194–201.

Mazenc, F., Pettersen, K., and Nijmeijer, H. (2002), "Global Uniform Asymptotic Stabilization of an Underactuated Surface Vessel," *IEEE Trans. on Automatic Control*, 47, 1759–1762.

Nguyen, T.D., Sørensen, A.J., and Quek, S.T. (2007), "Design of hybrid controller for dynamic positioning from calm to extreme sea conditions," *Automatica*, 43, 768–785.

Panagou, D., and Kyriakopoulos, K.J. (2011), "A switching control approach for the robust practical stabilization of a unicycle-like marine vehicle under non-vanishing perturbations," in *Proc. of the 2011 IEEE International Conference on Robotics and Automation*, May, Shanghai, P.R. China, pp. 1525–1530.

Panagou, D., Tanner, H.G., and Kyriakopoulos, K.J. (2011), "Control of nonholonomic systems using reference vector fields," in *Proc. of the 50th IEEE Conference on Decision and Control and European Control Conference*, Dec., Orlando, Florida, pp. 2831–2836.

Pereira, A., Das, J., and Sukhatme, G.S. (2008), "An Experimental Study of Station Keeping on an Underactuated ASV," in *Proc. of the 2008 IEEE/RSJ Int. Conf. on Intelligent Robots and Systems*, Sep., Nice, France, pp. 3164–3171.

Pettersen, K.Y., and Egeland, O. (1999), "Time-Varying Exponential Stabilization of the Position and Attitude of an Underactuated Autonomous Underwater Vehicle," *IEEE Trans. on Automatic Control*, 44, 112–115.

Pettersen, K.Y., and Fossen, T.I. (2000), "Underactuated Dynamic Positioning of a Ship - Experimental Results," *IEEE Trans. on Control Systems Technology*, 8, 856–863.

Pettersen, K.Y., and Nijmeijer, H. (2001), "Semi-Global Practical Stabilization and Disturbance Adaptation for an Underactuated Ship," *Modeling, Identification and Control*, 22, 89–101.

Refsnes, J.E., Sorensen, A.J., and Pettersen, K.Y. (2007), "Output feedback control of slender body underwater vehicles with current estimation," *International Journal of Control*, 80, 1136–1150.

Refsnes, J.E., Sorensen, A.J., and Pettersen, K.Y. (2008), "Model-based output feedback control of slender-body underactuated AUVs: Theory and Experiments," *IEEE Trans. on Control and Systems Technology*, 16, 930–946.

Reyhanoglu, M. (1996), "Control and Stabilization of an Underactuated Surface Vessel," in *Proc. of the 35th IEEE Conf. on Decision and Control*, Dec., Kobe, Japan, pp. 2371–2376.

Sørensen, A.J., Sagatun, S.I., and Fossen, T.I. (1996), "Design of a Dynamic Positioning System Using Model-Based Control," *Control Engineering Practice*, 4, 359–368.

Sørensen, A.J. (2011), "A survey of dynamic positioning control systems," *Annual Reviews in Control*, 35, 123–136.

Tannuri, E.A., Agostinho, A.C., Morishita, H.M., and Jr, L.M. (2010), "Dynamic positioning systems: An experimental analysis of sliding mode control," *Control Engineering Practice*, 18, 1121–1132.

Wang, W., and Clark, C.M. (2006), "Modeling and Simulation of the VideoRay Pro III Underwater Vehicle," in *Proc. of OCEANS 2006 - Asia Pacific*, May, Singapore, pp. 1–7.

Wichlund, K.Y., Sordalen, O.J., and Egeland, O. (1995), "Control of Vehicles with second-order constraints: Underwater Vehicles," in *Proc. of the 3rd European Conf. on Control*, Sep., Rome, Italy, pp. 3086–3091.

Zhao, J., and Hill, D.J. (2008), "On stability, L_2-gain and H_∞ control for switched systems," *Automatica*, 44, 1220–1232.

Appendix A: Proof of Theorem 5.1

Proof In order to study the convergence of the position trajectories $\boldsymbol{r}(t)$ into a ball around the origin, we think of the system Σ_1 as decomposed into two subsystems with different time scales, where the state $\boldsymbol{z} \triangleq [\psi \;\; v_r]^\top$ constitutes the boundary-layer (fast) system, and the states $\boldsymbol{x} \triangleq [x \;\; y]^\top$ constitute the reduced (slow) system. Then, the closed-loop dynamics under the control law (4b) of the overall system Σ_1 can be written as a singular perturbation model by considering the (small) parameter $\epsilon \triangleq \frac{1}{k_2}$, for k_2 sufficiently large, as follows:

$$\begin{aligned}
\dot{x} &= u_r \cos\psi - v_r \sin\psi + V_c \cos\beta_c \\
\dot{y} &= u_r \sin\psi + v_r \cos\psi + V_c \sin\beta_c \\
\epsilon\dot{\psi} &= -(\psi - \phi) \\
\epsilon\dot{v}_r &= \frac{m_{11}}{m_{22}} u_r(\psi - \phi) + \epsilon\frac{Y_v}{m_{22}} v_r + \epsilon\frac{Y_{v|v|}}{m_{22}} |v_r|\, v_r.
\end{aligned}$$

The boundary-layer system has one isolated root, given for $\epsilon = 0$ as $\psi = \phi$. Taking $\eta = \psi - \phi$, one can easily verify that $\epsilon\frac{d\eta}{dt} = \epsilon\dot{\psi} - \epsilon\dot{\phi} = -(\psi - \phi) - \epsilon\dot{\phi} \Rightarrow \frac{d\eta}{d\tau} \triangleq -\eta$, where $\epsilon\frac{d\eta}{dt} = \frac{d\eta}{d\tau}$ (Khalil 2002). This implies that ψ converges exponentially and at a very fast time scale to ϕ.

Let us now consider the candidate Lyapunov function $V = \frac{1}{2}(x^2 + y^2)$ for the reduced (slow) subsystem, which is positive definite, radially unbounded and of class C^1, and take the derivative of V along the system trajectories, evaluated at the stable equilibrium $\eta = 0$ of the boundary-layer subsystem, i.e. for $\psi = \phi$:

$$\dot{V} = \nabla V \begin{bmatrix} \dot{x} \\ \dot{y} \end{bmatrix} = \begin{bmatrix} x & y \end{bmatrix} \begin{bmatrix} u_r \cos\phi - v_r \sin\phi + V_c \cos\beta_c \\ u_r \sin\phi + v_r \cos\phi + V_c \sin\beta_c \end{bmatrix} = \boldsymbol{r}^\top \begin{bmatrix} \cos\phi \\ \sin\phi \end{bmatrix} u_r + \boldsymbol{r}^\top \begin{bmatrix} -\sin\phi \\ \cos\phi \end{bmatrix} v_r + \boldsymbol{r}^\top \begin{bmatrix} V_c \cos\beta_c \\ V_c \sin\beta_c \end{bmatrix}.$$

Substituting the control law (4a) yields:

$$\begin{aligned}
\dot{V} &= -k_1 \left(\boldsymbol{r}^\top \begin{bmatrix} \cos\phi \\ \sin\phi \end{bmatrix}\right) \operatorname{sgn}\left(\boldsymbol{r}^\top \begin{bmatrix} \cos\phi \\ \sin\phi \end{bmatrix}\right) \|\boldsymbol{r}\| - \left(\boldsymbol{r}^\top \begin{bmatrix} \cos\phi \\ \sin\phi \end{bmatrix}\right) \operatorname{sgn}(\boldsymbol{p}^\top \boldsymbol{r}) \|\boldsymbol{v}\| + \boldsymbol{r}^\top \begin{bmatrix} -\sin\phi \\ \cos\phi \end{bmatrix} v_r + \boldsymbol{r}^\top \boldsymbol{v} \\
&= -k_1 \left|\boldsymbol{r}^\top \begin{bmatrix} \cos\phi \\ \sin\psi \end{bmatrix}\right| \|\boldsymbol{r}\| - \left(\boldsymbol{r}^\top \begin{bmatrix} \cos\phi \\ \sin\phi \end{bmatrix}\right) \operatorname{sgn}(\boldsymbol{p}^\top \boldsymbol{r}) \|\boldsymbol{v}\| + \boldsymbol{r}^\top \begin{bmatrix} -\sin\phi \\ \cos\phi \end{bmatrix} v_r + \boldsymbol{r}^\top \boldsymbol{v}.
\end{aligned}$$

Let us check the sign of $\dot{V}$ by considering the following cases.

Case 1: $\operatorname{sgn}(\boldsymbol{p}^\top \boldsymbol{r}) = -1$ and $\boldsymbol{r}^\top \boldsymbol{v} \geq 0$, see Fig. A1. Then:

$$\dot{V} = -k_1 \left|\boldsymbol{r}^\top \begin{bmatrix} \cos\phi \\ \sin\phi \end{bmatrix}\right| \|\boldsymbol{r}\| + \left(\boldsymbol{r}^\top \begin{bmatrix} \cos\phi \\ \sin\phi \end{bmatrix}\right) \|\boldsymbol{v}\| + \boldsymbol{r}^\top \begin{bmatrix} -\sin\phi \\ \cos\phi \end{bmatrix} v_r + |\boldsymbol{r}^\top \boldsymbol{v}|.$$

In this case, one can easily verify out of Fig. A1 that $\boldsymbol{r}^\top \begin{bmatrix} \cos\phi \\ \sin\phi \end{bmatrix} \leq 0$. Therefore:

$$\dot{V} = -k_1 \left|\boldsymbol{r}^\top \begin{bmatrix} \cos\phi \\ \sin\phi \end{bmatrix}\right| \|\boldsymbol{r}\| - \left|\boldsymbol{r}^\top \begin{bmatrix} \cos\phi \\ \sin\phi \end{bmatrix}\right| \|\boldsymbol{v}\| + \boldsymbol{r}^\top \begin{bmatrix} -\sin\phi \\ \cos\phi \end{bmatrix} v_r + |\boldsymbol{r}^\top \boldsymbol{v}|.$$

After some algebra one can verify that:

$$\left|\boldsymbol{r}^\top \begin{bmatrix} \cos\phi \\ \sin\phi \end{bmatrix}\right| = \frac{1}{\|\mathbf{F}\|} \left|\boldsymbol{r}^\top \begin{bmatrix} \mathrm{F}_{px} \\ \mathrm{F}_{py} \end{bmatrix}\right| \overset{(3)}{=} \frac{1}{\|\mathbf{F}\|} \left(x^2 + y^2\right) |\boldsymbol{r}^\top \hat{\boldsymbol{v}}| = |\boldsymbol{r}^\top \hat{\boldsymbol{v}}|, \tag{A1}$$

where the norm of the vector field is $\|\mathbf{F}\| \triangleq \sqrt{\mathrm{F}_{px}^2 + \mathrm{F}_{py}^2} \overset{(3)}{=} x^2 + y^2$, and $\hat{\boldsymbol{v}} = [\cos\beta_c \;\; \sin\beta_c]^\top$

is the unit vector along the current direction. Consequently, one has:

$$\begin{aligned}\dot{V} &\overset{(A1)}{=} -k_1|\boldsymbol{r}^\top\hat{\boldsymbol{v}}|\|\boldsymbol{r}\| - |\boldsymbol{r}^\top\hat{\boldsymbol{v}}|\|\boldsymbol{v}\| + \boldsymbol{r}^\top\begin{bmatrix}-\sin\phi\\ \cos\phi\end{bmatrix}v_r + |\boldsymbol{r}^\top\hat{\boldsymbol{v}}|\|\boldsymbol{v}\| \\ &= -k_1|\boldsymbol{r}^\top\hat{\boldsymbol{v}}|\|\boldsymbol{r}\| + \boldsymbol{r}^\top\begin{bmatrix}-\sin\phi\\ \cos\phi\end{bmatrix}v_r \leq -k_1|\boldsymbol{r}^\top\hat{\boldsymbol{v}}|\|\boldsymbol{r}\| + \|\boldsymbol{r}\||v_r|. \end{aligned} \tag{A2}$$

Case 2: $\mathrm{sgn}(\boldsymbol{p}^\top\boldsymbol{r}) = -1$ and $\boldsymbol{r}^\top\boldsymbol{v} < 0$. Then:

$$\dot{V} = -k_1\left|\boldsymbol{r}^\top\begin{bmatrix}\cos\phi\\ \sin\phi\end{bmatrix}\right|\|\boldsymbol{r}\| + \left(\boldsymbol{r}^\top\begin{bmatrix}\cos\phi\\ \sin\phi\end{bmatrix}\right)\|\boldsymbol{v}\| + \boldsymbol{r}^\top\begin{bmatrix}-\sin\phi\\ \cos\phi\end{bmatrix}v_r - |\boldsymbol{r}^\top\boldsymbol{v}|.$$

In this case one has $\boldsymbol{r}^\top\begin{bmatrix}\cos\phi\\ \sin\phi\end{bmatrix} \leq 0$. Therefore:

$$\begin{aligned}\dot{V} &= -k_1\left|\boldsymbol{r}^\top\begin{bmatrix}\cos\phi\\ \sin\phi\end{bmatrix}\right|\|\boldsymbol{r}\| - \left|\boldsymbol{r}^\top\begin{bmatrix}\cos\phi\\ \sin\phi\end{bmatrix}\right|\|\boldsymbol{v}\| + \boldsymbol{r}^\top\begin{bmatrix}-\sin\phi\\ \cos\phi\end{bmatrix}v_r - \left|\boldsymbol{r}^\top\boldsymbol{v}\right| \\ &= -\left|\boldsymbol{r}^\top\begin{bmatrix}\cos\phi\\ \sin\phi\end{bmatrix}\right|(k_1\|\boldsymbol{r}\| + \|\boldsymbol{v}\|) + \boldsymbol{r}^\top\begin{bmatrix}-\sin\phi\\ \cos\phi\end{bmatrix}v_r - \left|\boldsymbol{r}^\top\boldsymbol{v}\right| \\ &\overset{(A1)}{=} -|\boldsymbol{r}^\top\hat{\boldsymbol{v}}|\,(k_1\|\boldsymbol{r}\| + \|\boldsymbol{v}\|) + \boldsymbol{r}^\top\begin{bmatrix}-\sin\phi\\ \cos\phi\end{bmatrix}v_r - \left|\boldsymbol{r}^\top\hat{\boldsymbol{v}}\right|\|\boldsymbol{v}\| \\ &= -|\boldsymbol{r}^\top\hat{\boldsymbol{v}}|\,(k_1\|\boldsymbol{r}\| + 2\|\boldsymbol{v}\|) + \boldsymbol{r}^\top\begin{bmatrix}-\sin\phi\\ \cos\phi\end{bmatrix}v_r \leq -|\boldsymbol{r}^\top\hat{\boldsymbol{v}}|\,(k_1\|\boldsymbol{r}\| + 2\|\boldsymbol{v}\|) + \|\boldsymbol{r}\||v_r|. \end{aligned} \tag{A3}$$

Case 3: $\mathrm{sgn}(\boldsymbol{p}^\top\boldsymbol{r}) = 1$ and $\boldsymbol{r}^\top\boldsymbol{v} \geq 0$. Then:

$$\dot{V} = -k_1\left|\boldsymbol{r}^\top\begin{bmatrix}\cos\phi\\ \sin\phi\end{bmatrix}\right|\|\boldsymbol{r}\| - \left(\boldsymbol{r}^\top\begin{bmatrix}\cos\phi\\ \sin\phi\end{bmatrix}\right)\|\boldsymbol{v}\| + \boldsymbol{r}^\top\begin{bmatrix}-\sin\phi\\ \cos\phi\end{bmatrix}v_r + |\boldsymbol{r}^\top\boldsymbol{v}|.$$

In this case one has $\boldsymbol{r}^\top\begin{bmatrix}\cos\phi\\ \sin\phi\end{bmatrix} \geq 0$. Therefore:

$$\begin{aligned}\dot{V} &= -k_1\left|\boldsymbol{r}^\top\begin{bmatrix}\cos\phi\\ \sin\phi\end{bmatrix}\right|\|\boldsymbol{r}\| - \left|\boldsymbol{r}^\top\begin{bmatrix}\cos\phi\\ \sin\phi\end{bmatrix}\right|\|\boldsymbol{v}\| + \boldsymbol{r}^\top\begin{bmatrix}-\sin\phi\\ \cos\phi\end{bmatrix}v_r + |\boldsymbol{r}^\top\boldsymbol{v}| \\ &\overset{(A1)}{=} -k_1|\boldsymbol{r}^\top\hat{\boldsymbol{v}}|\|\boldsymbol{r}\| - |\boldsymbol{r}^\top\hat{\boldsymbol{v}}|\|\boldsymbol{v}\| + \boldsymbol{r}^\top\begin{bmatrix}-\sin\phi\\ \cos\phi\end{bmatrix}v_r + |\boldsymbol{r}^\top\hat{\boldsymbol{v}}|\|\boldsymbol{v}\| = -k_1|\boldsymbol{r}^\top\hat{\boldsymbol{v}}|\|\boldsymbol{r}\| + \boldsymbol{r}^\top\begin{bmatrix}-\sin\phi\\ \cos\phi\end{bmatrix}v_r, \end{aligned}$$

i.e. $\dot{V}$ is the same as in Case 1.

Case 4: $\mathrm{sgn}(\boldsymbol{p}^\top\boldsymbol{r}) = 1$ and $\boldsymbol{r}^\top\boldsymbol{v} < 0$. Then:

$$\dot{V} = -k_1\left|\boldsymbol{r}^\top\begin{bmatrix}\cos\phi\\ \sin\phi\end{bmatrix}\right|\|\boldsymbol{r}\| - \left(\boldsymbol{r}^\top\begin{bmatrix}\cos\phi\\ \sin\phi\end{bmatrix}\right)\|\boldsymbol{v}\| + \boldsymbol{r}^\top\begin{bmatrix}-\sin\phi\\ \cos\phi\end{bmatrix}v_r - |\boldsymbol{r}^\top\boldsymbol{v}|.$$

In this case one has $\boldsymbol{r}^\top\begin{bmatrix}\cos\phi\\ \sin\phi\end{bmatrix} \geq 0$. Therefore:

$$\begin{aligned}\dot{V} &= -k_1\left|\boldsymbol{r}^\top\begin{bmatrix}\cos\phi\\ \sin\phi\end{bmatrix}\right|\|\boldsymbol{r}\| - \left|\boldsymbol{r}^\top\begin{bmatrix}\cos\phi\\ \sin\phi\end{bmatrix}\right|\|\boldsymbol{v}\| + \boldsymbol{r}^\top\begin{bmatrix}-\sin\phi\\ \cos\phi\end{bmatrix}v_r - |\boldsymbol{r}^\top\boldsymbol{v}| \\ &\overset{(A1)}{=} -k_1|\boldsymbol{r}^\top\hat{\boldsymbol{v}}|\|\boldsymbol{r}\| - |\boldsymbol{r}^\top\hat{\boldsymbol{v}}|\|\boldsymbol{v}\| + \boldsymbol{r}^\top\begin{bmatrix}-\sin\phi\\ \cos\phi\end{bmatrix}v_r - |\boldsymbol{r}^\top\hat{\boldsymbol{v}}|\|\boldsymbol{v}\| = -|\boldsymbol{r}^\top\hat{\boldsymbol{v}}|\,(k_1\|\boldsymbol{r}\| + 2\|\boldsymbol{v}\|) + \boldsymbol{r}^\top\begin{bmatrix}-\sin\phi\\ \cos\phi\end{bmatrix}v_r, \end{aligned}$$

i.e. $\dot{V}$ is the same as in Case 2.

As expected, the evolution of $\dot{V}$ along the system trajectories $\dot{x}(t)$, $\dot{y}(t)$ depends on the unactuated dynamics via the sway velocity v_r. Furthermore, since v_r comes from the control input $\zeta = u_r r$, one can resort to an input-to-state stability (ISS) argument to study its evolution, as

follows: Consider the candidate ISS-Lyapunov function $V_v = \frac{1}{2}{v_r}^2$ and take its time derivative

$$\dot{V}_v = -\frac{m_{11}}{m_{22}} v_r(u_r r) - \left(\frac{|Y_v|}{m_{22}} {v_r}^2 + \frac{|Y_{v|v|}|}{m_{22}} |v_r| \, {v_r}^2 \right),$$

where $Y_v, Y_{v|v|} < 0$ and the function $w(v_r) = \frac{|Y_v|}{m_{22}} {v_r}^2 + \frac{|Y_{v|v|}|}{m_{22}} |v_r| \, {v_r}^2$ is positive definite. Take $\theta \in (0,1)$, then:

$$\dot{V}_v = -\frac{m_{11}}{m_{22}} v_r(u_r r) - (1-\theta) w(v_r) - \theta w(v_r) \Rightarrow \dot{V}_v \leq -(1-\theta) w(v_r), \; \forall v_r : -\frac{m_{11}}{m_{22}} v_r(u_r r) - \theta w(v_r) \leq 0.$$

If the control input $\zeta = u_r r$ is bounded, $|\zeta| \leq \zeta_b$, then

$$\dot{V}_v \leq -(1-\theta) w(v_r), \; \forall |v_r| : |Y_v||v_r| + |Y_{v|v|}||v_r|^2 > \frac{m_{11}}{\theta} \zeta_b.$$

Then, the subsystem (1e) is ISS w.r.t. ζ (Khalil 2002, Thm 4.19), which essentially expresses that for any bounded input $\zeta = u_r r$, the linear velocity $v_r(t)$ will be ultimately bounded by a class $\mathcal{K}$ function of $\sup_{t>0} |\zeta(t)|$. If furthermore $\zeta(t) = u_r(t) r(t)$ converges to zero as $t \to \infty$, then $v_r(t)$ converges to zero as well (Khalil 2002).

At this point, note that the control input $r \triangleq -k_2 \eta$ is bounded and converges to zero at a very fast time scale, since the orientation error $\eta = 0$ is the exponentially stable equilibrium of the boundary-layer subsystem. This further implies that, for sufficiently large k_2, the sway velocity v_r converges to zero very fast, compared to the remaining slow dynamics of $x(t)$, $y(t)$. Consequently, the positive terms in (A2), (A3) vanish much faster than the negative terms, yielding $\dot{V} \leq 0$, where $\dot{V} = 0$ if $\boldsymbol{r}^\top \hat{\boldsymbol{v}} = 0$ or if $\boldsymbol{r} = \boldsymbol{0}$.

Consequently, for $\boldsymbol{r}^\top \boldsymbol{v} \neq 0$, any initial $\boldsymbol{r}(0)$ and any $0 < r_0 < \|\boldsymbol{r}(0)\|$, one has that $\dot{V}$ is negative in the set $\{\boldsymbol{r} \mid \frac{1}{2}{r_0}^2 \leq V(\|\boldsymbol{r}\|) \leq \frac{1}{2}\|\boldsymbol{r}(0)\|^2\}$, which verifies that $\boldsymbol{r}(t)$ enters the set $\{\boldsymbol{r} \mid V(\boldsymbol{r}) \leq \frac{1}{2}{r_0}^2\}$, or equivalently, $\boldsymbol{r}(t)$ enters the ball $\mathcal{B}(\boldsymbol{0}, r_0)$. Finally, note that the case $\boldsymbol{r}^\top \hat{\boldsymbol{v}} = 0$ where $\dot{V} = 0$ does not affect the convergence of the system into $\mathcal{B}(\boldsymbol{0}, r_0)$, since the system can not identically stay in this set. □

Appendix B: Proof of Theorem 5.2

Proof Under the control law (5) the system trajectories $\boldsymbol{q}(t)$ first reach the boundary $\partial G_{1_{G_2}}$, and then reach the boundary ∂G_{2_B}.

To verify the first argument, i.e. that the system trajectories reach the boundary $\partial G_{1_{G_2}}$, consider the Lyapunov-like function:

$$V_{21} = \boldsymbol{r}^\top \boldsymbol{v} + \frac{1}{2}(\psi - \phi_p)^2 = V_c(x \cos\beta_c + y \sin\beta_c) + \frac{1}{2}(\psi - \phi_p)^2,$$

which is positive everywhere in G_1, since there one has $\boldsymbol{r}^\top \boldsymbol{v} \geq 0$, and becomes zero on the boundary $\partial G_{1_{G_2}}$ for $\psi = \phi_p$, and take its time derivative along the system trajectories:

$$\begin{aligned} \dot{V}_{21} &= \left[\begin{smallmatrix} V_c \cos\beta_c & V_c \sin\beta_c \end{smallmatrix}\right] \left[\begin{smallmatrix} \dot{x} \\ \dot{y} \end{smallmatrix}\right] + (\psi - \phi_p)\dot{\psi} \overset{(1)}{=} \boldsymbol{v}^\top \left[\begin{smallmatrix} \cos\psi \\ \sin\psi \end{smallmatrix}\right] u_r + \boldsymbol{v}^\top \left[\begin{smallmatrix} -\sin\psi \\ \cos\psi \end{smallmatrix}\right] v_r + \|\boldsymbol{v}\|^2 + (\psi - \phi_p) r \\ &\overset{(5)}{=} -k_3 \operatorname{sgn}(\cos\beta_c) \|\boldsymbol{v}\| \boldsymbol{v}^\top \left[\begin{smallmatrix} \cos\psi \\ \sin\psi \end{smallmatrix}\right] + \boldsymbol{v}^\top \left[\begin{smallmatrix} -\sin\psi \\ \cos\psi \end{smallmatrix}\right] v_r + \|\boldsymbol{v}\|^2 - k_4(\psi - \phi_p)^2. \end{aligned}$$

Let us consider the following cases.

(1) $\mathrm{sgn}(\cos\beta_c) = -1$. It is reasonable to assume that, under the control law (4), the vehicle has reached G_1 with $\boldsymbol{v}^\top \left[\begin{smallmatrix}\cos\psi\\ \sin\psi\end{smallmatrix}\right] < 0$. Then:

$$\begin{aligned}\dot{V}_{21} &= -k_3 \left|\boldsymbol{v}^\top \left[\begin{smallmatrix}\cos\psi\\ \sin\psi\end{smallmatrix}\right]\right| \|\boldsymbol{v}\| + \|\boldsymbol{v}\|^2 + \boldsymbol{v}^\top \left[\begin{smallmatrix}-\sin\psi\\ \cos\psi\end{smallmatrix}\right] v_r - k_4(\psi-\phi_p)^2 = \\ &= \|\boldsymbol{v}\| \left(\|\boldsymbol{v}\| - k_3 \left|\boldsymbol{v}^\top \left[\begin{smallmatrix}\cos\psi\\ \sin\psi\end{smallmatrix}\right]\right|\right) + \boldsymbol{v}^\top \left[\begin{smallmatrix}-\sin\psi\\ \cos\psi\end{smallmatrix}\right] v_r - k_4(\psi-\phi_p)^2,\end{aligned}$$

where the first term is < 0 for $\|\boldsymbol{v}\| < k_3 \left|\boldsymbol{v}^\top \left[\begin{smallmatrix}\cos\psi\\ \sin\psi\end{smallmatrix}\right]\right| \Rightarrow k_3 > 1$. Furthermore, one has that $\zeta = u_r r \to 0$, since $r \to 0$ (via $\psi \to (\phi_p = \psi_e)$), yielding $v_r \to 0$. Note also that $\dot{V}_{21} = 0 \Leftrightarrow \{k_3 = 1 \text{ and } v_r = 0 \text{ and } \psi = \phi_p\}$. Therefore, for $k_3 > 1$ the system trajectories starting in G_1 enter the region G_2.

(2) $\mathrm{sgn}(\cos\beta_c) = 1$. Similarly one can take $\boldsymbol{v}^\top \left[\begin{smallmatrix}\cos\psi\\ \sin\psi\end{smallmatrix}\right] > 0$ and follow the same procedure to yield that for $k_3 > 1$, the system trajectories starting in G_1 enters the region G_2.

Finally, to verify the second argument, i.e. that the system trajectories reach the boundary ∂G_{2_B}, consider the Lyapunov-like function:

$$V_{22} = {r_0}^2 - \|\boldsymbol{r}\|^2 = {r_0}^2 - (x^2 + y^2),$$

which is positive for $\boldsymbol{r} \in G_2$ and zero on ∂G_{2_B}, and take its time derivative along the system trajectories:

$$\begin{aligned}\dot{V}_{22} &= -2\boldsymbol{r}^\top \left[\begin{smallmatrix}\cos\psi\\ \sin\psi\end{smallmatrix}\right] u_r - 2\boldsymbol{r}^\top \left[\begin{smallmatrix}-\sin\psi\\ \cos\psi\end{smallmatrix}\right] v_r - 2\boldsymbol{r}^\top \boldsymbol{v} \\ &\overset{(5)}{=} 2\boldsymbol{r}^\top \left[\begin{smallmatrix}\cos\psi\\ \sin\psi\end{smallmatrix}\right] \mathrm{sgn}(\cos\beta_c) k_3 \|\boldsymbol{v}\| - 2\boldsymbol{r}^\top \left[\begin{smallmatrix}-\sin\psi\\ \cos\psi\end{smallmatrix}\right] v_r - 2\boldsymbol{r}^\top \boldsymbol{v}.\end{aligned}$$

Let us consider the following cases.

(1) $\mathrm{sgn}(\cos\beta_c) = -1$, then one has: $\boldsymbol{r}^\top \boldsymbol{v} < 0$ and $\boldsymbol{r}^\top \left[\begin{smallmatrix}\cos\psi\\ \sin\psi\end{smallmatrix}\right] > 0$. Consequently:

$$\begin{aligned}\dot{V}_{22} &= -2k_3 \boldsymbol{r}^\top \left[\begin{smallmatrix}\cos\psi\\ \sin\psi\end{smallmatrix}\right] \|\boldsymbol{v}\| - 2\boldsymbol{r}^\top \left[\begin{smallmatrix}-\sin\psi\\ \cos\psi\end{smallmatrix}\right] v_r - 2\boldsymbol{r}^\top \boldsymbol{v} = \\ &- 2k_3 \left|\boldsymbol{r}^\top \left[\begin{smallmatrix}\cos\psi\\ \sin\psi\end{smallmatrix}\right]\right| \|\boldsymbol{v}\| - 2\boldsymbol{r}^\top \left[\begin{smallmatrix}-\sin\psi\\ \cos\psi\end{smallmatrix}\right] v_r + 2\left|\boldsymbol{r}^\top \boldsymbol{v}\right| \\ &\le -2k_3 \left|\boldsymbol{r}^\top \left[\begin{smallmatrix}\cos\psi\\ \sin\psi\end{smallmatrix}\right]\right| \|\boldsymbol{v}\| - 2\boldsymbol{r}^\top \left[\begin{smallmatrix}-\sin\psi\\ \cos\psi\end{smallmatrix}\right] v_r + 2\|\boldsymbol{r}\|\|\boldsymbol{v}\| \\ &= 2\|\boldsymbol{v}\| \left(\|\boldsymbol{r}\| - k_3 \left|\boldsymbol{r}^\top \left[\begin{smallmatrix}\cos\psi\\ \sin\psi\end{smallmatrix}\right]\right|\right) - 2\boldsymbol{r}^\top \left[\begin{smallmatrix}-\sin\psi\\ \cos\psi\end{smallmatrix}\right] v_r,\end{aligned}$$

where the first term is < 0 for $\|\boldsymbol{r}\| < k_3 \left|\boldsymbol{r}^\top \left[\begin{smallmatrix}\cos\psi\\ \sin\psi\end{smallmatrix}\right]\right| \le \|\boldsymbol{r}\| \Rightarrow k_3 > 1$. Thus, for $k_3 > 1$, the system trajectories $\boldsymbol{q}(t)$ hit the boundary ∂G_{2_B} and enters B.

(2) $\mathrm{sgn}(\cos\beta_c) = 1$, then one has: $\boldsymbol{r}^\top \boldsymbol{v} < 0$ and $\boldsymbol{r}^\top \left[\begin{smallmatrix}\cos\psi\\ \sin\psi\end{smallmatrix}\right] < 0$. Following the same procedure, one eventually gets that $\dot{V}_{22} < 0 \Rightarrow k_3 > 1$.

□

Appendix C: Proof of Theorem 5.3

Proof Let us first prove that the system trajectories enter the set G_1, by considering the candidate Lyapunov-like function $V_{31} = -\boldsymbol{r}^\top \boldsymbol{v}$, which is positive for $\boldsymbol{r} \in G_2$ and zero on $\partial G_{2_{G_1}}$. The time derivative along the system trajectories is:

$$\begin{aligned}\dot{V}_{31} &\overset{(1)}{=} -V_c \cos\beta_c (u_r \cos\psi - v_r \sin\psi + V_c \cos\beta_c) - V_c \sin\beta_c (u_r \sin\psi + v_r \cos\psi + V_c \sin\beta_c) \\ &\overset{(6)}{=} -\|\boldsymbol{v}\|^2 - \boldsymbol{v}^\top \begin{bmatrix} -\sin\psi \\ \cos\psi \end{bmatrix} v_r,\end{aligned}$$

where $v_r \to 0$ since $\zeta = u_r r \to 0$. Consequently, the system trajectories $\boldsymbol{q}(t)$ enter the set G_1. Finally, for $\boldsymbol{r} \in G_1$ take the candidate Lyapunov-like function $V_{32} = {r_0}^2 - x^2 - y^2$, where

$$\dot{V}_{32} = -\|\boldsymbol{v}\|^2 - \boldsymbol{v}^\top \begin{bmatrix} -\sin\psi \\ \cos\psi \end{bmatrix} v_r < 0,$$

to verify that the system trajectories $\boldsymbol{q}(t)$ enter the set A. □

Appendix D: Proof of Theorem 5.6

Proof Under the feedback linearization transformation (8), the corresponding dynamic equations (1d), (1f) read $\dot{u}_r = \alpha$, $\dot{r} = \beta$, respectively, where α, β are the new control inputs. Consider the candidate Lyapunov function

$$V_\tau = \frac{1}{2}\left(u_r - u_{r,d}(\cdot)\right)^2 + \frac{1}{2}\left(r - r_d(\cdot)\right)^2,$$

and take its time derivative as $\dot{V}_\tau = (u_r - u_{r,d}(\cdot))\left(\dot{u}_r - (\nabla u_{r,d}(\cdot))\dot{\boldsymbol{q}}\right) + (r - r_d(\cdot))\left(\dot{r} - (\nabla r_d(\cdot))\dot{\boldsymbol{q}}\right)$.

Then, under the control inputs (9) one gets

$$\dot{V}_\tau = -k_u (u_r - u_{r_d}(\cdot))^2 - k_r (r - r_d(\cdot))^2 \leq -2\min\{k_u, k_r\} V_\tau,$$

which verifies that the actual velocities $u_r(t)$, $r(t)$ are GES to the virtual velocities $u_{r,d}(\cdot)$, $r_d(\cdot)$, respectively. □

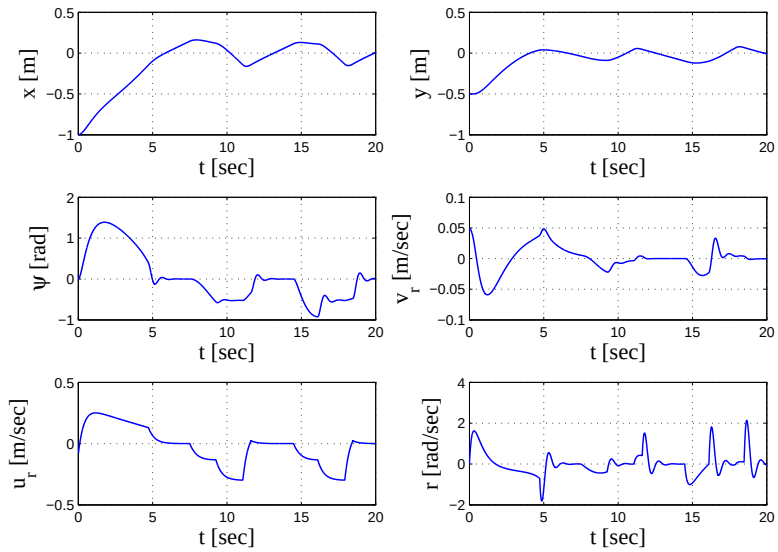

(a) The system trajectories $x(t), y(t), \psi(t), v_r(t), u_r(t), r(t)$

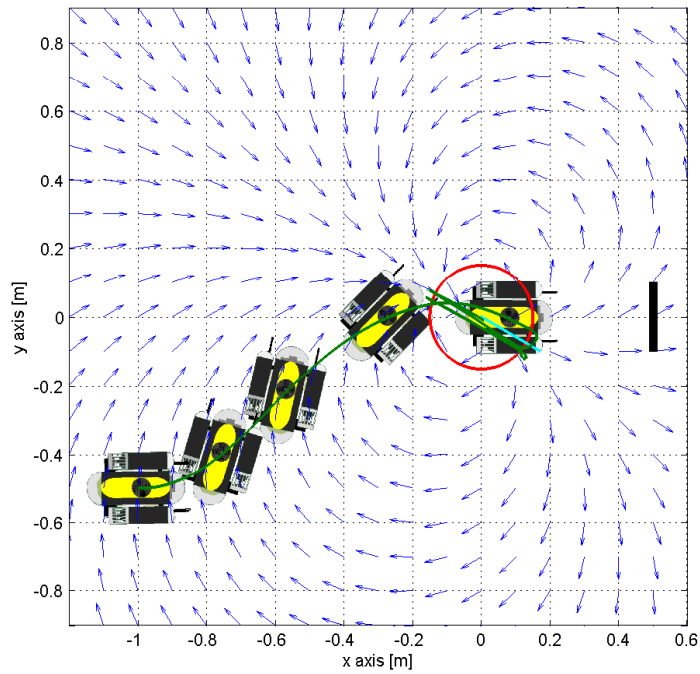

(b) The path $x(t), y(t)$ followed by the vehicle

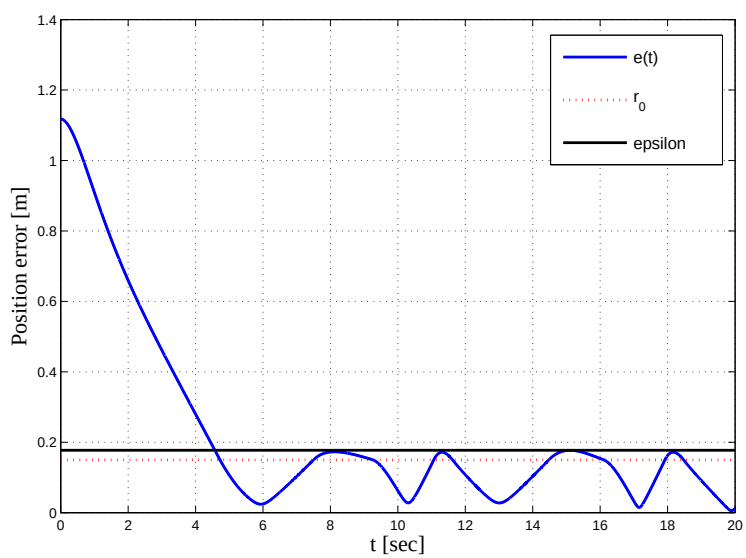

(c) The position error $e(t) = \sqrt{x(t)^2 + y(t)^2}$

Figure 4. System response for **known** $V_c = 0.1$ m/sec, $\beta_c = -30$ deg.

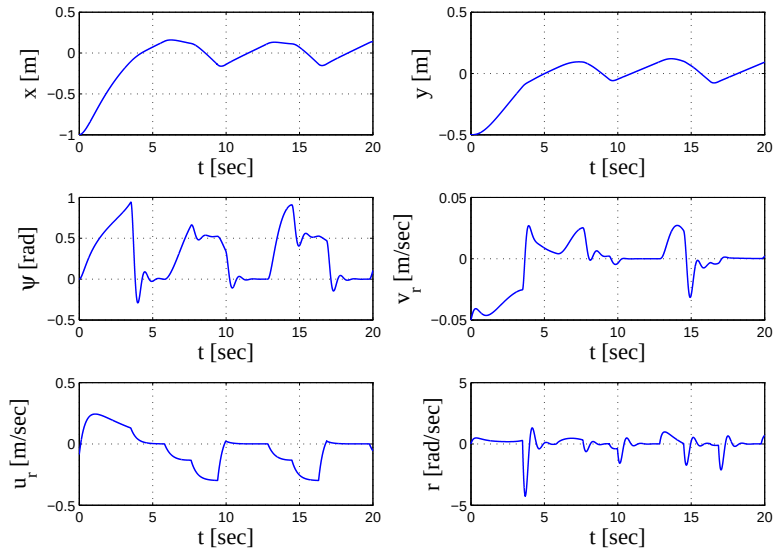

(a) The system trajectories $x(t), y(t), \psi(t), v_r(t), u_r(t), r(t)$

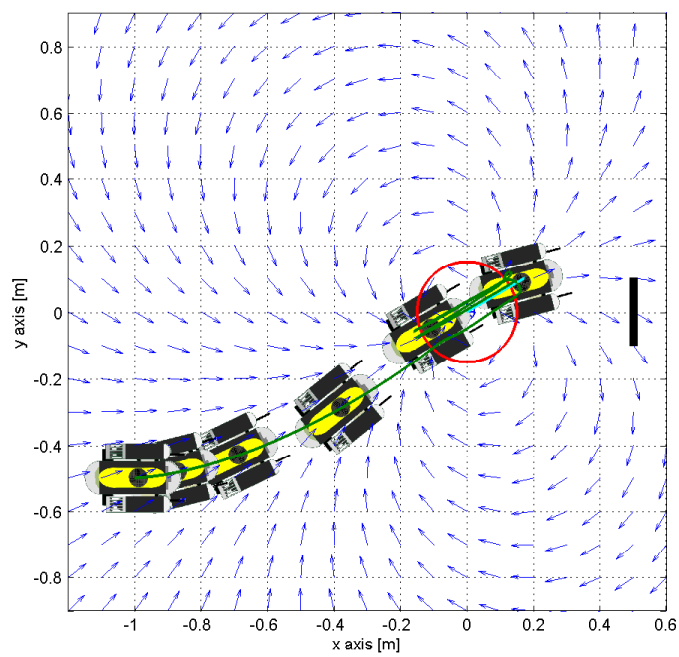

(b) The path $x(t), y(t)$ followed by the vehicle

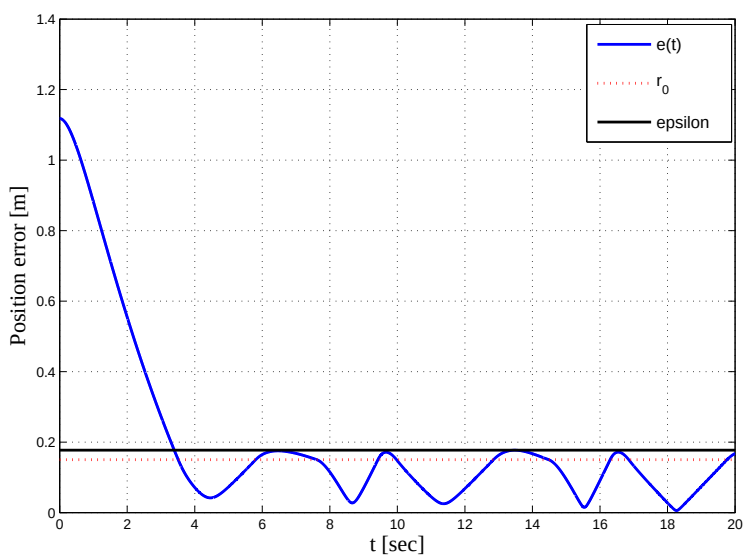

(c) The position error $e(t) = \sqrt{x(t)^2 + y(t)^2}$

Figure 5. System response for **known** $V_c = 0.1$ m/sec, $\beta_c = 30$ deg.

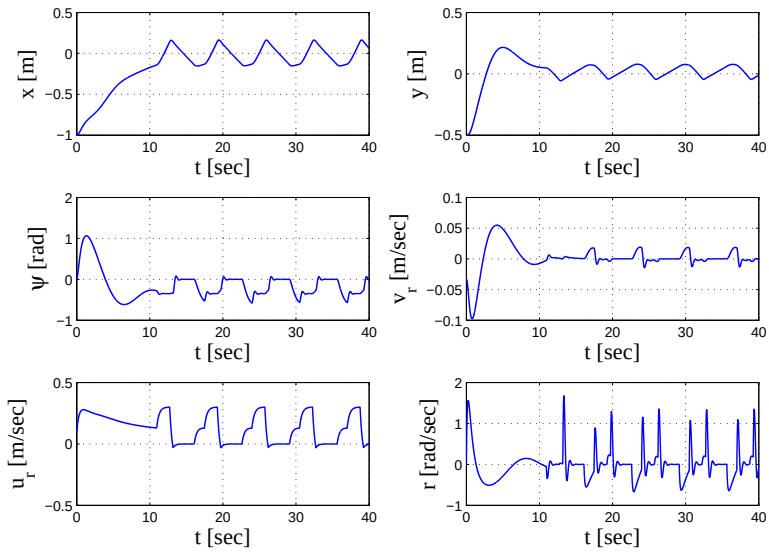

(a) The system trajectories $x(t), y(t), \psi(t), v_r(t), u_r(t), r(t)$

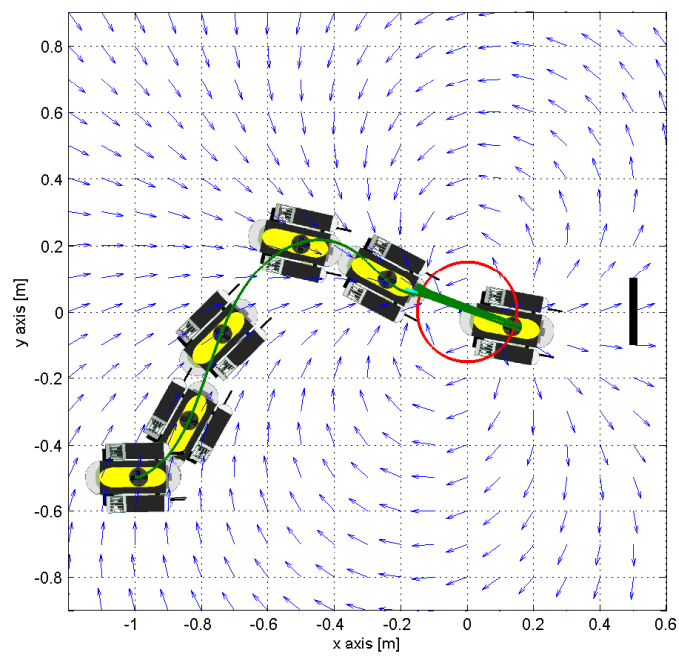

(b) The path $x(t), y(t)$ followed by the vehicle

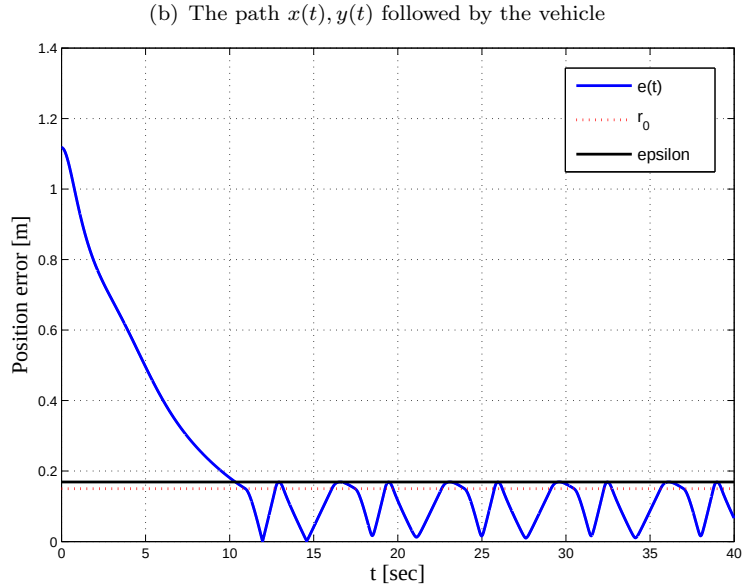

(c) The position error $e(t) = \sqrt{x(t)^2 + y(t)^2}$

Figure 6. System response for **known** $V_c = 0.1$ m/sec, $\beta_c = 160$ deg.

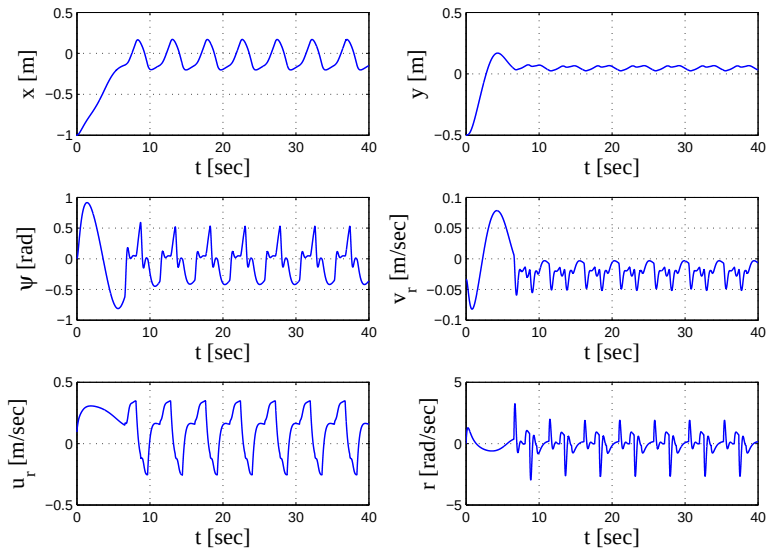

(a) The system trajectories $x(t), y(t), \psi(t), v_r(t), u_r(t), r(t)$

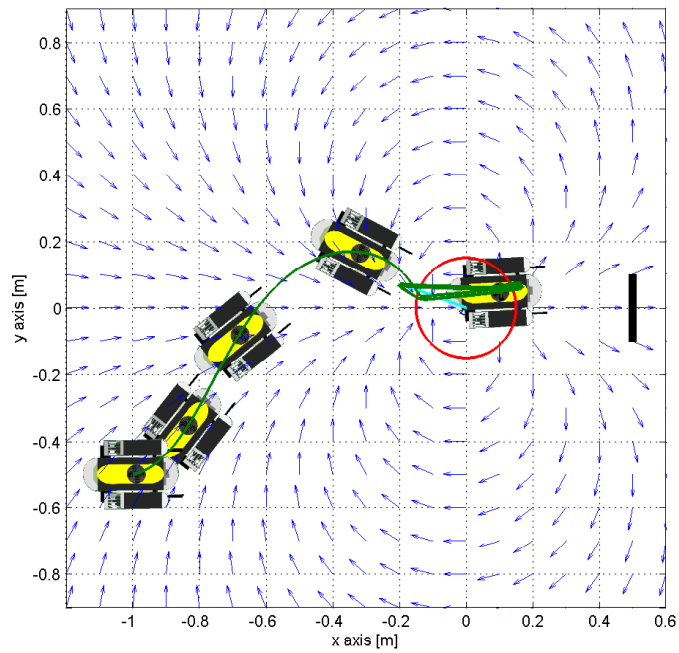

(b) The path $x(t), y(t)$ followed by the vehicle

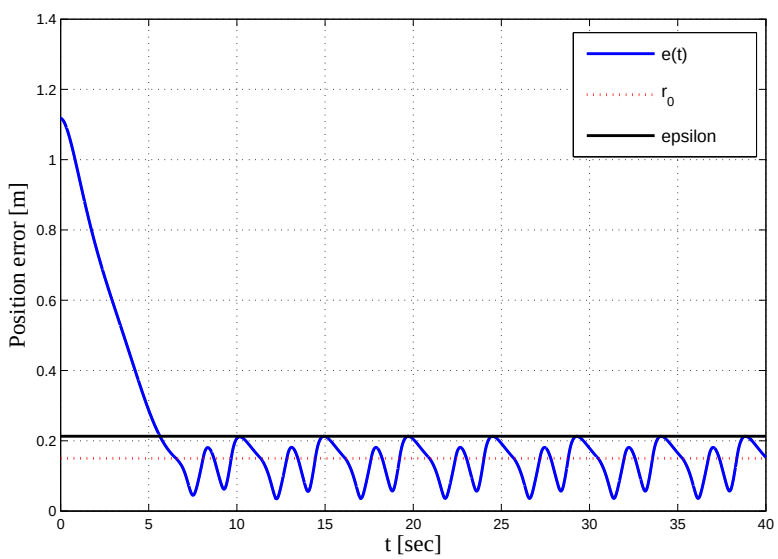

(c) The position error $e(t) = \sqrt{x(t)^2 + y(t)^2}$

Figure 7. System response for $V_c = 0.1$ m/sec and **unknown** $\beta_c = 160$ deg.

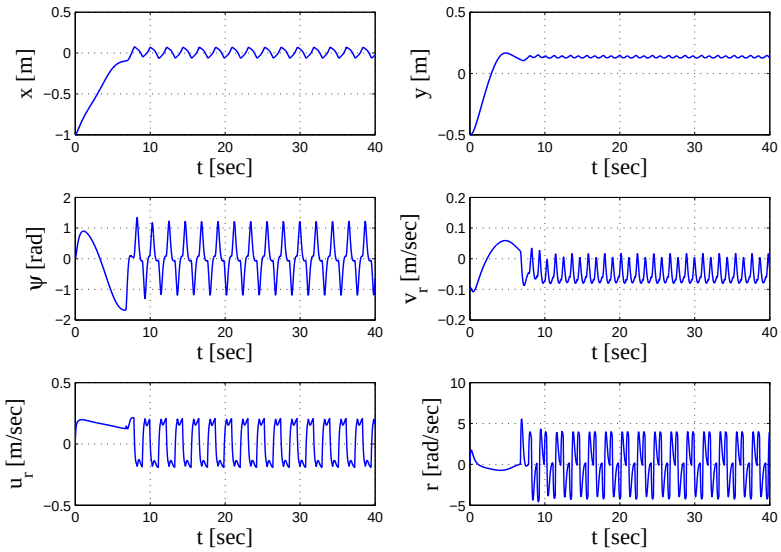

(a) The system trajectories $x(t), y(t), \psi(t), v_r(t), u_r(t), r(t)$

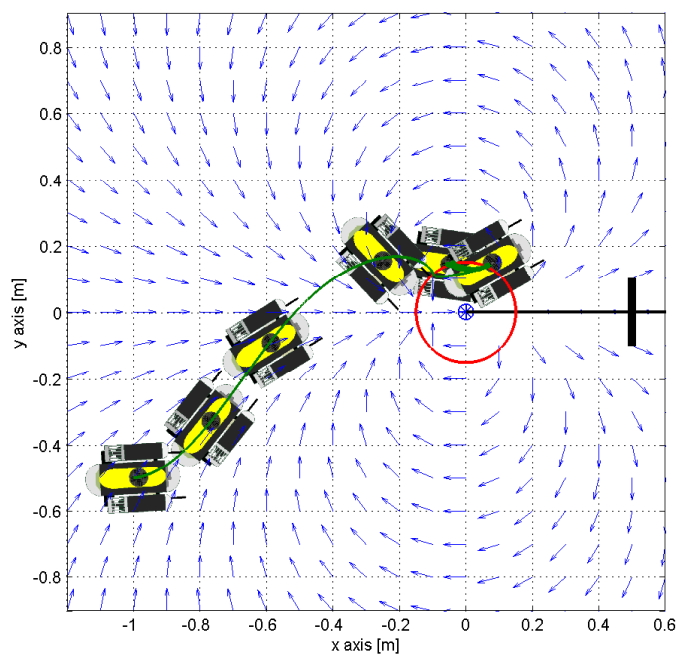

(b) The path $x(t), y(t)$ followed by the closed loop system

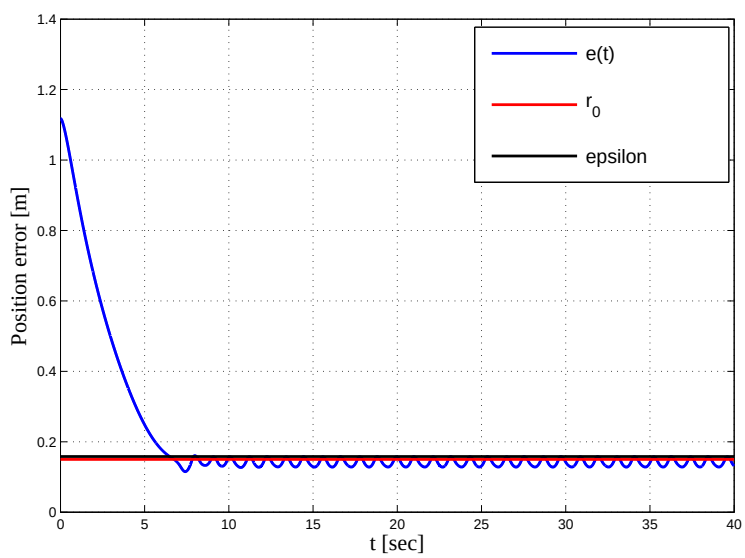

(c) The position error $e(t) = \sqrt{x(t)^2 + y(t)^2}$

Figure 8. System response for $V_c = 0.1$ m/sec and **unknown** $\beta_c = 90$ deg.

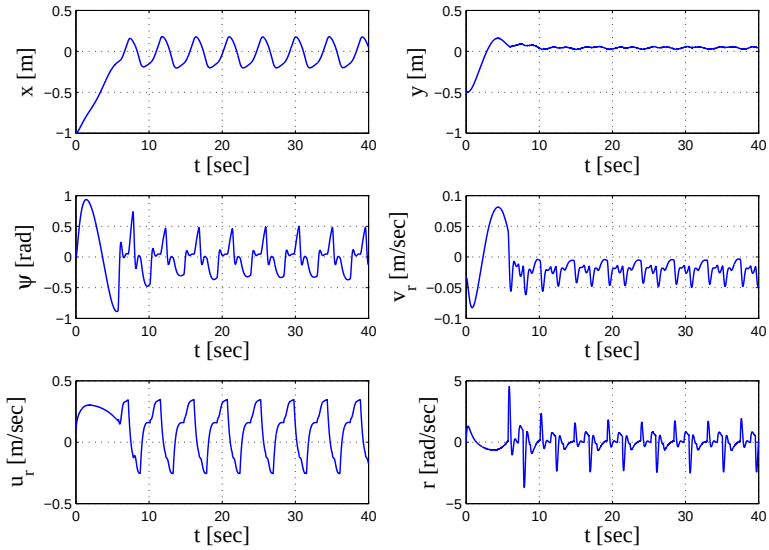

(a) The system trajectories $x(t), y(t), \psi(t), v_r(t), u_r(t), r(t)$

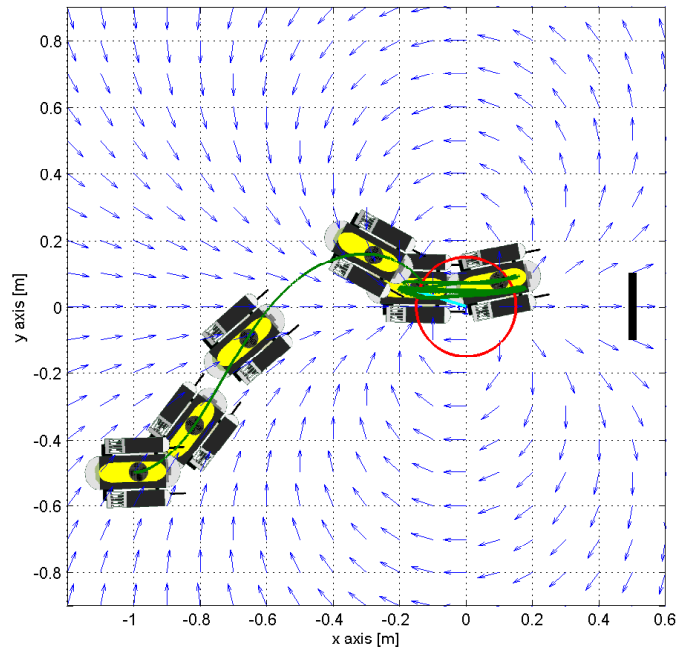

(b) The path $x(t), y(t)$ followed by the closed loop system

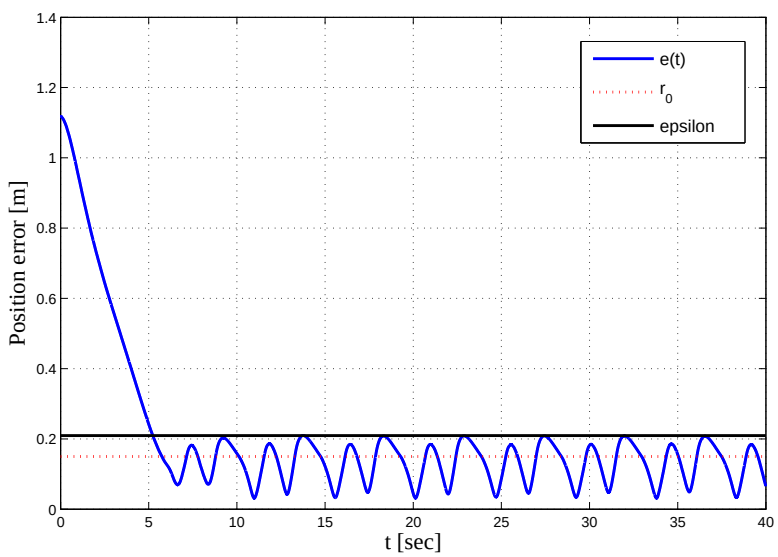

(c) The position error $e(t) = \sqrt{x(t)^2 + y(t)^2}$

Figure 9. System response for *unknown* $\boldsymbol{v}$, such that $\|\boldsymbol{v}\|_{\max} = 0.1$ m/sec, under **varying** current direction β_c.

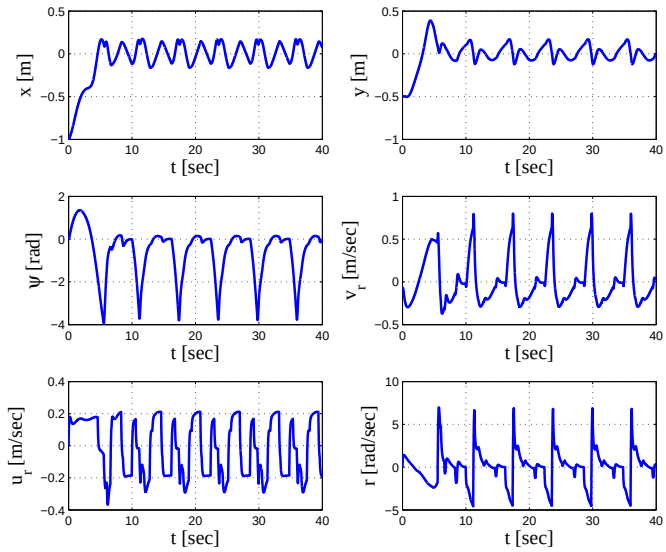

(a) The system trajectories $x(t), y(t), \psi(t), v_r(t), u_r(t), r(t)$

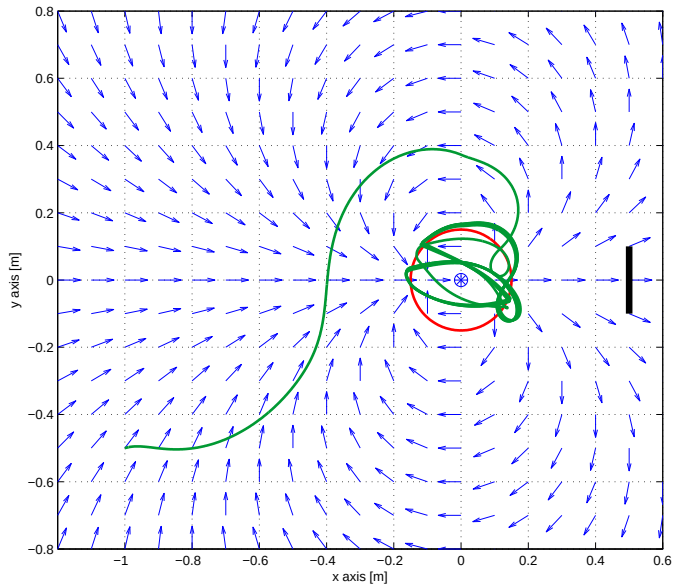

(b) The path $x(t), y(t)$ followed by the closed loop system

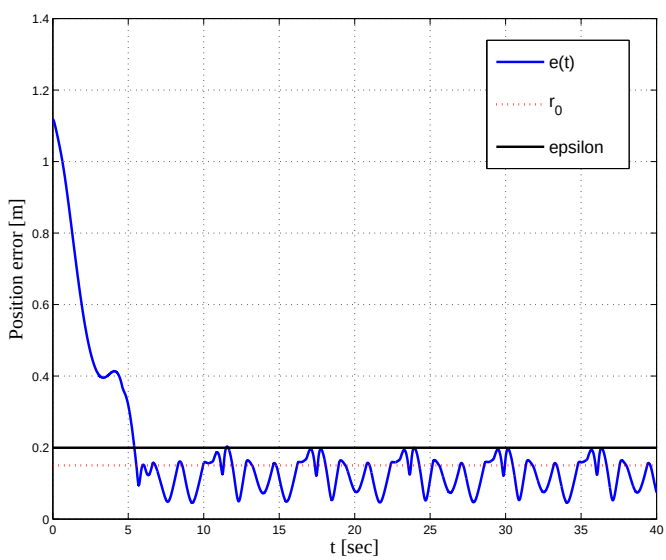

(c) The position error $e(t) = \sqrt{x(t)^2 + y(t)^2}$

Figure 10. System response for $V_c = 0.1$ m/sec and **unknown** $\beta_c = 90$ deg **with off-diagonal inertia and damping elements**.

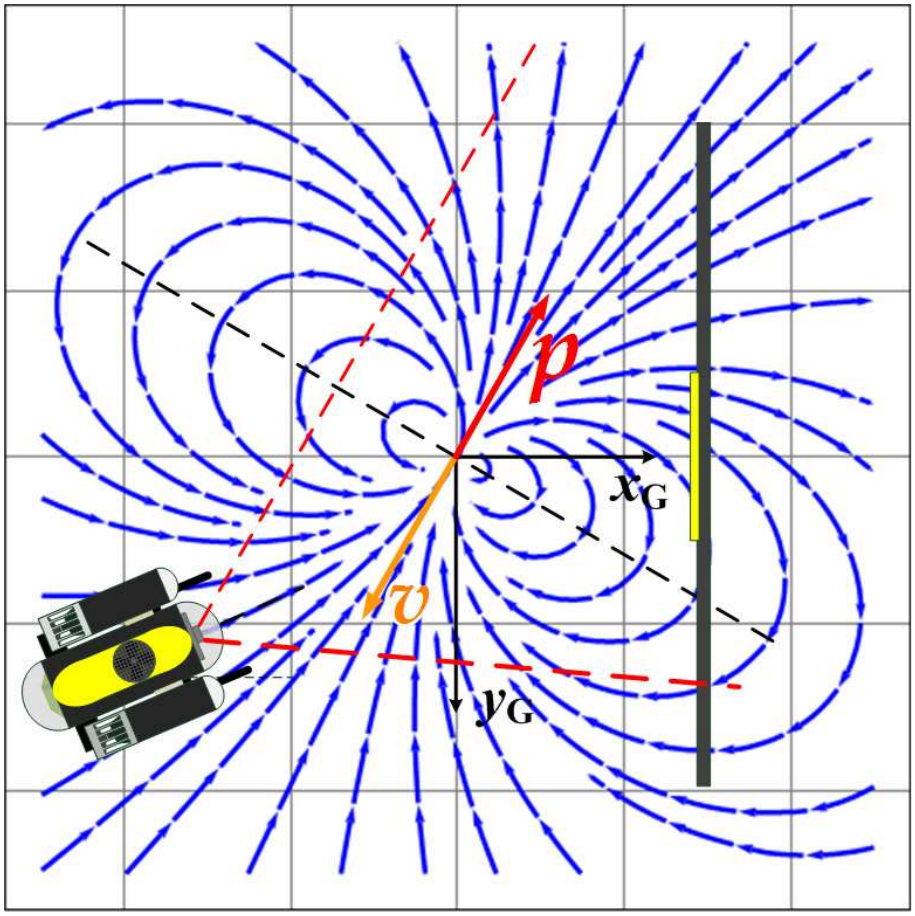

Figure A1. System configuration w.r.t. the dipolar field (3)